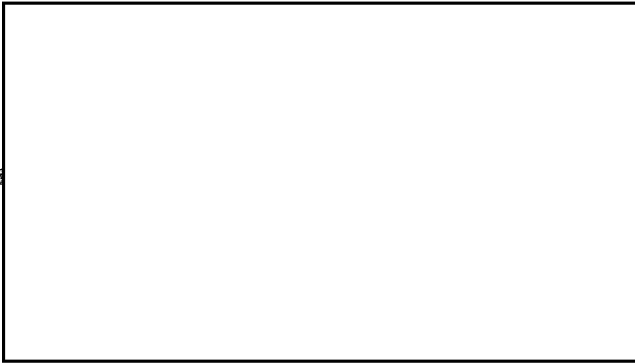


*Attachment 1*

STAT



STAT

TECHNICAL REPORT

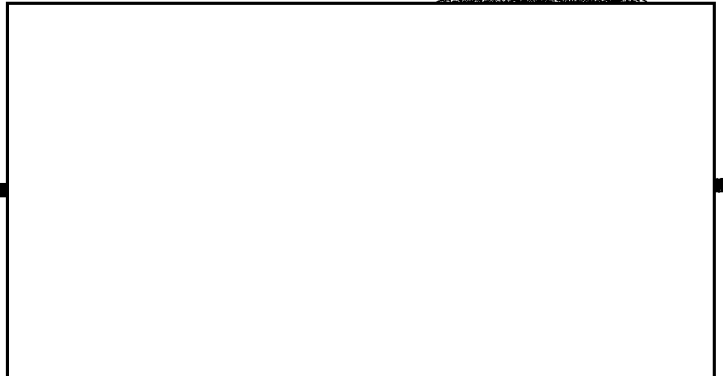


6 DECEMBER 1965

# **MULTIPLE IMAGE INTEGRATION VIEWER-PRINTER**

Phase 1—Feasibility Study

STAT



Declass Review by NGA.

STAT

STAT

TECHNICAL REPORT

6 DECEMBER 1965

# **MULTIPLE IMAGE INTEGRATION VIEWER - PRINTER**

Phase 1 - Feasibility Study

STAT

### SUMMARY

This report discusses the results of an introductory study of the problems of multiple image integration and the details of the proposed design for an experimental three-input integration viewer-printer. Automatic image correlation is used in the proposed equipment for rapid and accurate registration of the three inputs. The outputs consist of a real-time electronic display for monitoring purposes, and a high resolution, slow scan readout onto 4- by 5-inch film that will reproduce image detail of up to 100 lines per millimeter on the original material.

CONTENTS

1. Introduction . . . . .	1
2. Technical Considerations . . . . .	5
2.1 Image Registration . . . . .	5
2.2 Image Enhancement . . . . .	19
2.3 Modulation Transfer Function . . . . .	22
2.4 Comparison of Electronic and Optical Image Integration System . . . . .	29
3. General Description of Multiple Image Integration Viewer-Printer . . . . .	31
3.1 Control Panel . . . . .	31
3.2 Input Platen . . . . .	31
3.3 Optical System . . . . .	34
3.4 Correlation System . . . . .	38
3.5 Video Processing . . . . .	41
3.6 System Performance . . . . .	52
4. Bibliography . . . . .	55
Appendix—Linear Superimposition of Multiple Images . . . . .	57

TABLES

2-1 Maximum Tolerable Displacement Errors at 3 Percent Response . . . . .	7
2-2 Comparison of Electronic and Optical Image Integration Systems . . . . .	30
3-1 Input Magnification Ratios . . . . .	52

## FIGURES

1-1	Prime Transformations . . . . .	2
1-2	Types of Terrain Relief Displacements . . . . .	3
2-1	Resultant Amplitude of Two Displaced Sine Waves . . . . .	6
2-2	Typical Modulation Transfer Functions for Aerial Photography . . . . .	7
2-3	Effect of Image Displacement on Modulation Transfer Function . . . . .	8
2-4	Image Displacement Due to Tilt. . . . .	9
2-5	Residual Second-Order Displacement Error Due to Tilt Angle . . . . .	10
2-6	Residual Second-Order Distortion for 6-Inch Focal Length. . . . .	11
2-7	Residual Second-Order Distortion for 12-Inch Focal Length . . . . .	12
2-8	Residual Second-Order Distortion for 24-Inch Focal Length . . . . .	13
2-9	Residual Second-Order Distortion for 48-Inch Focal Length . . . . .	14
2-10	Residual Second-Order Distortion for 100-Inch Focal Length . . . . .	15
2-11	Residual Second-Order Distortion for 200-Inch Focal Length . . . . .	16
2-12	Correlator Transfer Functions . . . . .	18
2-13	Log Plot of Step Wedges in Sunlight and Shadow . . . . .	23
2-14	Linear Plot of Step Wedges in Sunlight and Shadow . . . . .	23
2-15	Modulation Transfer Functions for Cathode-Ray Tube and Image Dissector, Linear Plot . . . . .	26
2-16	Modulation Transfer Functions for Cathode-Ray Tube and Image Dissector, Logarithmic Plot . . . . .	28
3-1	General Configuration of Multiple Image Integration Viewer-Printer . . . . .	32
3-2	Block Diagram of Multiple Image Integration Viewer-Printer . . . . .	33
3-3	Control Panel. . . . .	34
3-4	Configuration of Input Platens . . . . .	35
3-5	Diagram of Optical System . . . . .	37
3-6	Lissajous Scan Generator. . . . .	39
3-7	One Channel of Video Correlator and Distortion Analyzer . . . . .	40
3-8	Block Diagram of Memory Unit . . . . .	41
3-9	Block Diagram of Modulator Circuits . . . . .	42
3-10	Block Diagram of a Single Image Dissector Channel . . . . .	43
3-11	Block Diagram of Variable Gamma Amplifier . . . . .	44
3-12	One Form of Nonlinear Amplifier . . . . .	44
3-13	Transfer Characteristic of Nonlinear Amplifier . . . . .	45
3-14	Results of Step Voltage Signal Applied to Input of Gamma Amplifier . . . . .	46
3-15	Video Signals . . . . .	47
3-16	Schematic Diagram of Experimental Gamma Amplifier . . . . .	49
3-17	Switching for Flicker Presentation. . . . .	51
3-18	Modulation Transfer Functions Referred to Image Dissector . . . . .	53
3-19	Theoretical Modulation Transfer Function of Complete System . . . . .	54

## 1. INTRODUCTION

Multiple image integration is the technique of utilizing several independent images of the same object as an aid to photographic interpretation. The improvement obtained in reliability and accuracy of interpretation may be due to any one or a combination of the following effects: (1) improvement in the contrast of low contrast images, due to the coherent addition of image detail and the noncoherent addition of grain or other random disturbances, (2) revelation of image detail hidden in shadows or missing due to other causes, by the superimposition of two or more inputs taken at different times of day or from different viewpoints, and (3) detection of changes due to human activity or natural causes, e.g., seasonal variations.

One of the major problems in image integration is that of superimposing the multiple images with sufficient accuracy to avoid loss of resolution, which would tend to offset any advantage gained by the increase in contrast or visibility of detail. Methods of image integration using optical superimposition have involved the use of multiple photographs taken at the same time from the same viewpoint. The improvement obtained is due solely to the integration of photographic grain, which theoretically improves image contrast by a factor of  $N^{1/2}$ , where  $N$  is the number of photographs integrated. The problem of superimposition is reduced in this case simply to that of physical alignment, since the inputs are all identical in scale and geometry.

To take advantage of all the benefits of image integration, however, photographs of different scale taken from different viewpoints must be used. Superimposition then involves computation of the geometrical transformations necessary to make the images congruent, followed by simultaneous implementation of these distortions on several images—a process similar to that required for stereo viewing of convergent oblique or panoramic photography.

The required transformations can be computed either from a knowledge of the acquisition parameters of the photography, or by simultaneous scanning of two or more inputs with subsequent correlation of the imagery. The latter method is of far greater practical interest. At present, electronic scanning is the only feasible method of point by point image correlation. The images to be integrated are scanned by identical patterns, and the image density variations converted into electrical video frequency waveforms. These waveforms are then compared in an electronic correlator, and the image transformations necessary to render the images congruent are computed. The image transformations can be implemented either optically or electronically by distorting the scanning patterns.

Image transformations can be analyzed into orders, depending on whether the image displacement involved is independent of the coordinates  $x$  and  $y$  measured from the center of the viewed area, or varies as  $x$ ,  $x^2$ ,  $x^3$ , etc.

Shifts in  $x$  and  $y$  which affect the entire image are zero-order transformations. There are four first-order transformations in which image displacement is proportional to  $x$  or  $y$ , and six second-order transformations in which image displacement is proportional to  $x^2$ ,  $y^2$ , or  $xy$ . These prime transformations are shown in Fig. 1-1.

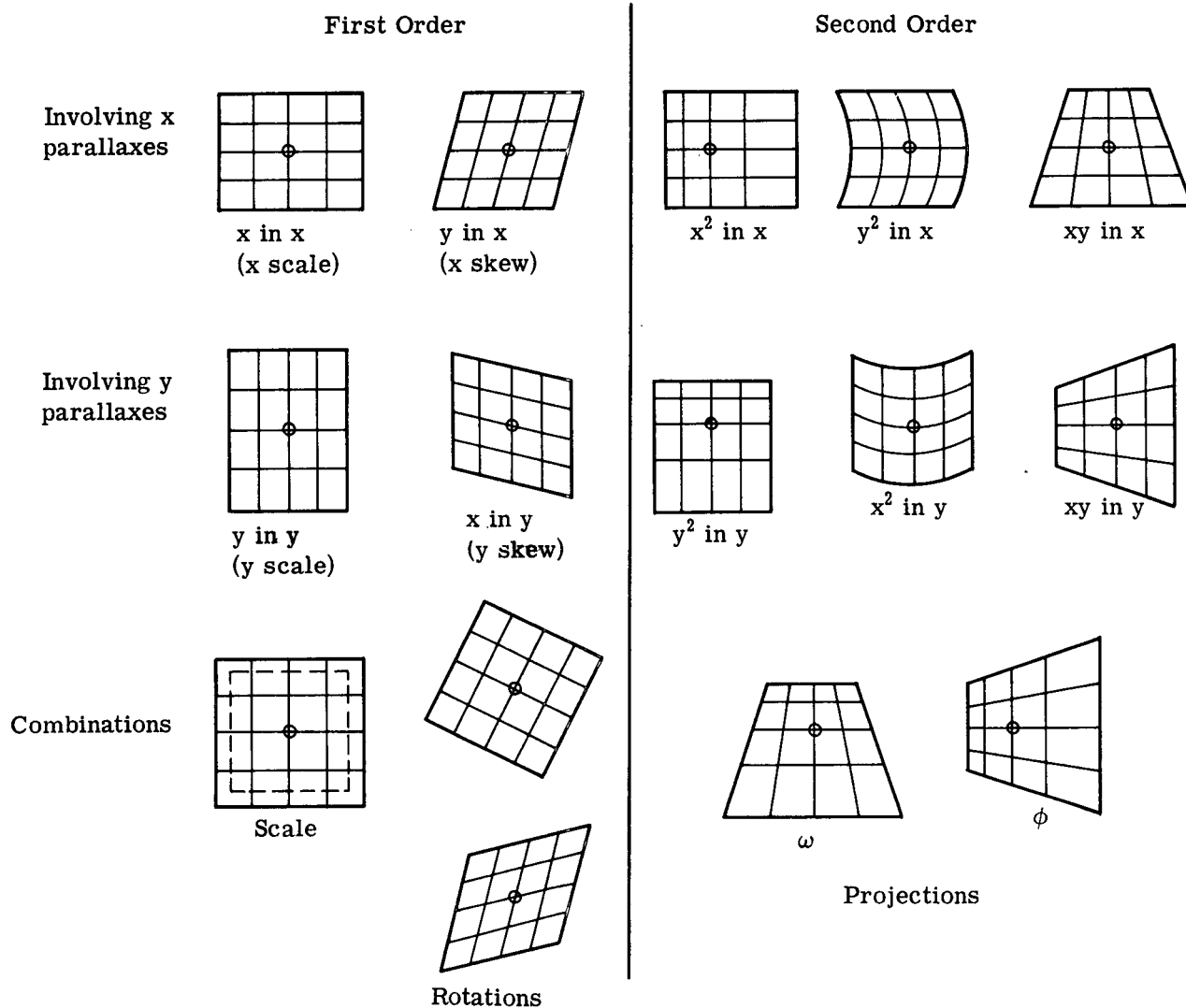


Fig. 1-1 — Prime transformations

The transformations to be applied to two images to obtain congruence depend not only on the viewpoint of the taking lens, but on the angular coverage of each image. Zero-order transformations (uniform displacements) are, of course, necessary whatever the image size. Similarly, first-order transformations such as scale, rotation, and skew, in which image displacement is proportional to the distance from the center of the viewed area, are necessary in all cases and must be increasingly accurate as the number of resolution elements in the field of view is increased.

Second-order distortions are present in every oblique photography. However, when only a small area is viewed, as is generally the case with an image integration viewer, the second-order distortion can be approximated with a straight line (first-order) correction. The superimposition errors involved in this process have been analyzed and are reported in Section 2.1.2.

Third-order effects are present in panoramic photography in the form of S curve and cubic scale distortion, but the magnitude of these effects has been found to be negligibly small when measured over the area of photography normally viewed.

Another form of image distortion must be considered in an image integration viewer, namely, high order terrain relief displacements. First-order transformations already discussed will correct for a constant terrain slope, as shown in Fig. 1-2a, while second-order transformations will correct simple curvature, as shown in Fig. 1-2b. Terrain relief due to cultural objects shows discontinuities in profile, as shown in Fig. 1-2c, corresponding to transformations which may reach as high as 100th order. It is obviously impossible to correct these displacements by using a systematic analysis, since the number of corrections to be applied would be astronomical. This problem is discussed further in Section 2.1.3.

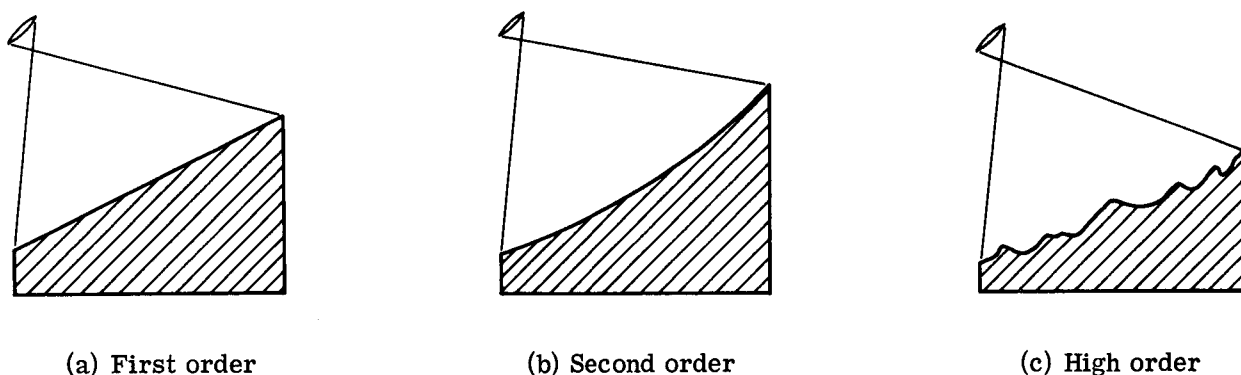


Fig. 1-2 — Types of terrain relief displacements

The next question to be considered is how the required transformations can be applied to the images. Of the ten possible first- and second-order transformations, only two (uniform scale and rotation) can be removed by conventional optical means. Correction of x and y scale variations and skew distortion requires the use of anamorphic optics. Second-order distortion due to obliquity can be corrected in an optical system by tilting the image and object planes with respect to the lens axis. The use of these techniques results in a very elaborate and expensive optical system which must be duplicated for each input channel of the image integration.

The problems associated with the use of optical systems for image superimposition lead to the consideration of electronic imaging systems. Image transformations can be produced relatively easily in an electronic system by changing the shape of the scanning pattern. Distortion of any order, including high order relief displacement, is capable of being corrected in this way.

Because an electronic system must be used in any case to scan and correlate the images and to compute the relative distortion, the use of electronic distortion removal techniques requires a minimum of additional equipment. The main criticism leveled at electronic imaging systems is their bandwidth restriction. There are, however, techniques by which this restriction can be overcome to the point where the output imagery is suitable for photointerpretive use.

Electronic imaging systems using scanning reduce the two-dimensional input imagery to a time varying video signal. Such a system is limited by three factors: (1) the size of the scanning spot or aperture relative to the area scanned, (2) the bandwidth of the electronic video channel, and (3) the size of the spot on the display tube relative to the area scanned. Factors 1 and 3 together determine the maximum number of resolution elements that can be reproduced, while factor 2 determines the maximum rate at which they can be reproduced.



Image pickup and display tubes exist which can handle  $9 \times 10^6$  image elements. This is equal to the maximum number of image elements that can be seen by the eye (at 5 line pairs per millimeter in a 12- by 12-inch photograph at a distance of 10 inches. To present this information at the normal rate of 30 frames per second would require a video bandwidth of 135 megacycles per second, which is beyond the state of the art. However, the only reason for a frame rate of 30 frames per second is to produce the illusion of image motion without flicker. In an image integration viewer, we are dealing only with static imagery. If a readout system using image storage is employed, the frame rate can be reduced to a few frames per second, and the full resolution capability of the pickup and display devices can be utilized with a video bandwidth as low as 20 megacycles per second, which is readily achieved. It should be noted that the capability of handling  $9 \times 10^6$  picture elements for electronic scanning devices approaches the performance of a lens. While highly optimized lenses may exceed this performance, normally used lenses are capable of reproducing about  $10^7$  image elements. Certain lenses in which compromises have to be made may fall below this figure. So far as the pickup and display devices are concerned, therefore, available electronic imaging systems come very close to matching optical systems. The overall resolution of either type of system is of course reduced by virtue of the use of several components in cascade.

Another aspect of image integration must be considered, namely, gamma control of the various inputs in general, and shadow suppression in particular. The use of input material taken under varying conditions of sunlight and in different seasons necessitates a correlation technique that ignores illumination conditions and the presence of heavy shadows, and operates only on physical objects. Since such objects are visible only by virtue of the illumination, this is not an easy task. The main problem is the presence of shadows; the ARES correlation circuit locks onto shadows very readily, which is quite acceptable when viewing stereo pairs obtained within a short time interval. In the image integration viewer, it is necessary to reduce the contrast between shadows and highlights for two reasons: (1) to enable images containing dissimilar shadow structure to be correlated, and (2) to reveal shadow detail present in the images. The contrast can be reduced by the use of nonlinear amplitude response (or gamma) in both the correlation and the viewing channels. A square root characteristic (gamma of 0.5) has been found effective in suppressing shadows. It should be pointed out that the optimum video processing characteristics for correlation and for viewing may not be the same. Therefore, we propose to use two independent gamma controls in each channel, one to optimize correlation and the other to optimize viewing.

As a result of the study program, design parameters for a three-input image integration viewer have been established. The instrument will accept three film chips of any size up to  $9\frac{1}{2}$  by  $9\frac{1}{2}$  inches. Correlation of the three inputs is achieved by electronic scanning using a 500-line, crossed diagonal scan. One input is designated as the master, and the geometry of the other two inputs is transformed in sequence into congruence with the master input. The necessary image transformations are stored in a memory. The scanned images are combined and displayed on a viewing monitor, which enables the video processing in each channel to be optimized in terms of tone reproduction and alignment.

When a satisfactory image has been built up, the system is switched to slow scan operation, and the integrated image is recorded on film at high resolution. The scan time is about 1 second.

## 2. TECHNICAL CONSIDERATIONS

### 2.1 IMAGE REGISTRATION

The first subject to be considered will be the required accuracy of registration. The distortion due to camera tilt will be analyzed next, to determine whether second-order corrections will be necessary in the image integration viewer. Finally, the effect of uncorrected relief parallax will be considered.

#### 2.1.1 Registration Accuracy

The effect of misregistration can be most easily evaluated by considering two sine-wave images, whose amplitudes,  $a$ , at any point,  $x$ , are

$$a_1 = A_1 \sin (2\pi f_1 x + \phi_1)$$

$$a_2 = A_2 \sin (2\pi F_2 x + \phi_2)$$

where  $A_1$  and  $A_2$  are the peak amplitudes, and  $f_1$  and  $f_2$  are the spatial frequencies. If the two images contain the same spatial frequencies, and if they are added, the resultant,  $R = a_1 + a_2$ , is given by

$$R^2 = (A_1 \cos \phi_1 + A_2 \cos \phi_2)^2 + (A_1 \sin \phi_1 + A_2 \sin \phi_2)^2$$

$$R = [A_1^2 + A_2^2 + 2A_1A_2 \cos (\phi_1 - \phi_2)]^{1/2}$$

The amplitude of the resulting image is therefore dependent on the phase angle, or displacement, between the two images.

The phase difference can be expressed as

$$\phi_1 - \phi_2 = 2\pi f \Delta x$$

where  $\Delta x$  is the displacement between images. When  $\Delta x = 0$ , the two images are perfectly aligned and the resultant amplitude is  $A_1 + A_2$ . When  $\Delta x = 1/4f$ , the sine waves are 90 degrees out of phase, and the resultant amplitude is  $(A_1^2 + A_2^2)^{1/2}$ . When  $\Delta x = 1/2f$ , the sine waves are 180 degrees out of phase, and the resultant amplitude is  $(A_1^2 - A_2^2)^{1/2}$ . The variation in amplitude of the combined sine wave is shown in Fig. 2-1 for  $A_1/A_2$  ratios of 1, 0.8, and 0.6. These curves can be used to determine the loss in modulation transfer function (MTF) due to the misalignment of images.

Fig. 2-2 shows typical MTF's for an aerial camera lens (Itek 24-inch,  $f/3.5$ ) and a high resolution film (type 4404). The combined MTF shows that the response is down to 50 percent at 50 cycles per millimeter, and down to 3 percent at 300 cycles per millimeter. Fig. 2-3 shows the

MTF resulting from two inputs, each having the combined MTF of Fig. 2-2, when the displacement,  $\Delta x$ , between them is equivalent to  $1/4$  wavelength and  $1/2$  wavelength, respectively, measured at a 300-cycle-per-millimeter spatial frequency. At less than a  $1/4$ -wavelength image displacement, the loss in MTF in most cases would be unimportant, whereas at image displacements of  $1/2$  wavelength and greater, the loss in MTF is quite noticeable.

On this basis, we can establish the maximum tolerable displacement error at about  $1/4f$ , where  $f$  is the spatial frequency at which the MTF of the system has dropped to 3 percent. The tolerable displacement error calculated on this basis is shown in Table 2-1.

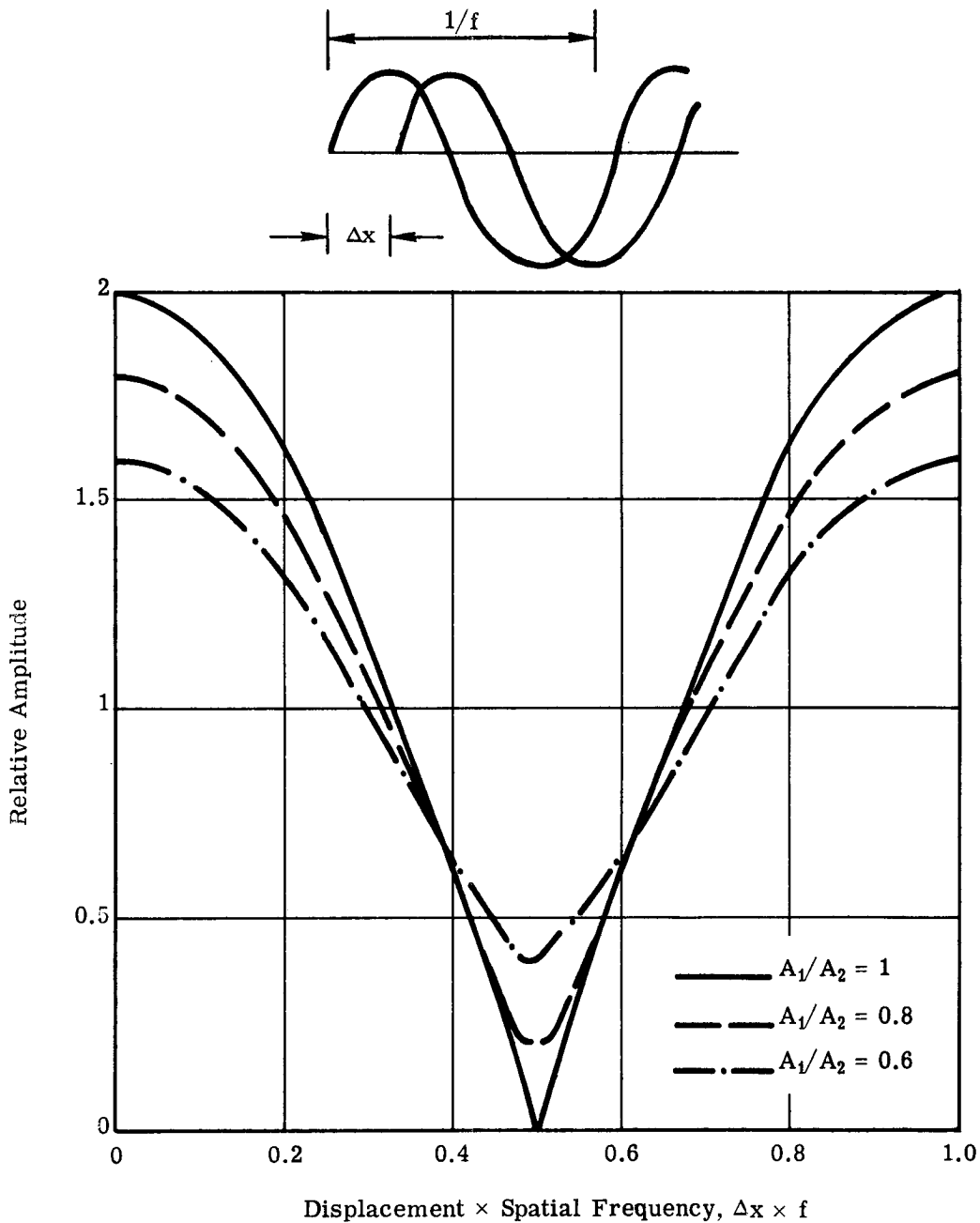
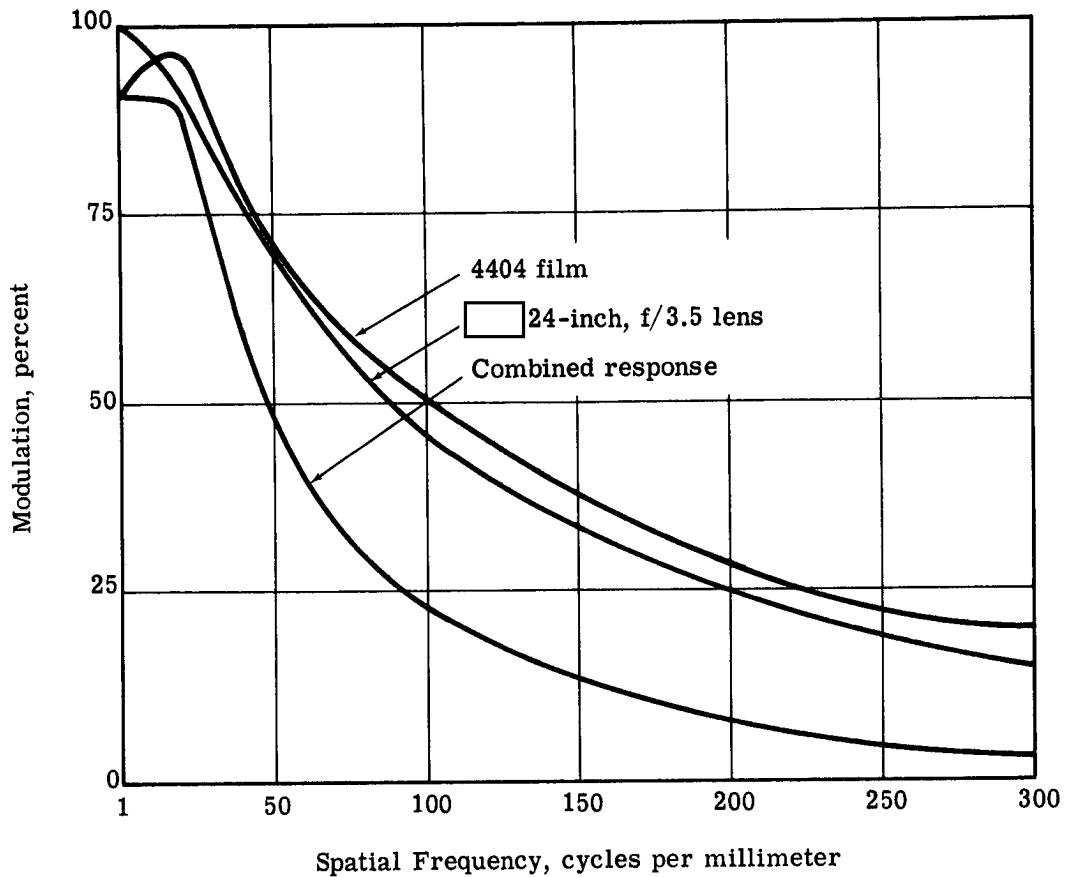


Fig. 2-1 — Resultant amplitude of two displaced sine waves



STAT

Fig. 2-2 — Typical modulation transfer functions for aerial photography

Table 2-1 — Maximum Tolerable Displacement Errors at 3 Percent Response

System Resolution at 3 Percent Response, lines per millimeter	Maximum Tolerable Displacement Error, microns
25	10.0
50	5.0
100	2.5
150	1.7
200	1.25

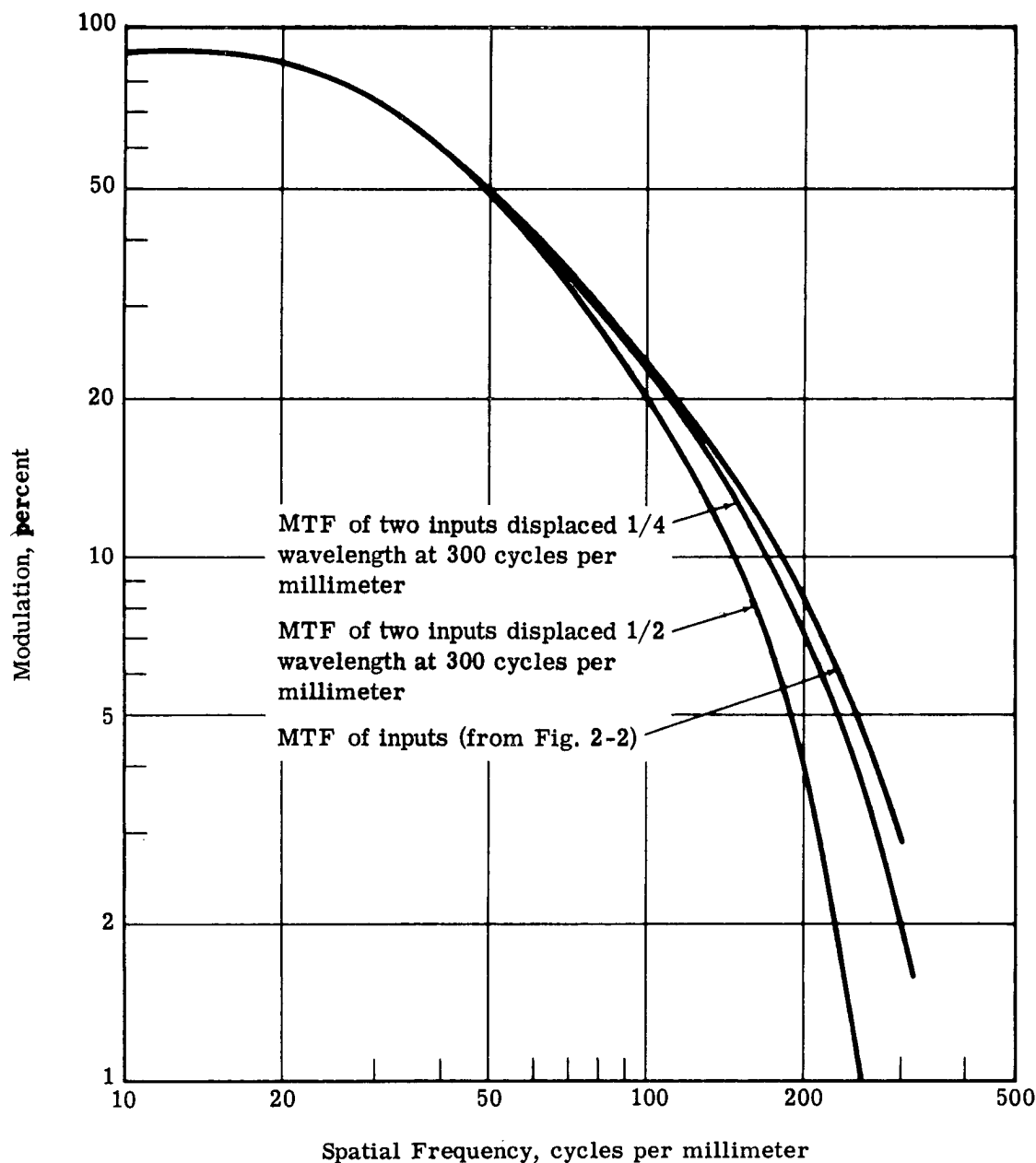


Fig. 2-3 — Effect of image displacement on modulation transfer function

### 2.1.2 Second-Order Distortions

Oblique and panoramic photography involve camera tilt angles that produce image distortion. The basic types of image distortion are shown in Fig. 1-1. Zero- and first-order distortions, i.e., scale, skew, and rotation, must always be corrected in order to superimpose images of any size. However, this is not the case with second-order distortions; the image displacements due to residual second-order distortion depend on the tilt angle and vary with the square of the y dimension of the image area examined. It is important in the present case to determine whether or not second-order corrections will be required in order to superimpose images to the required degree of accuracy, since this will be a major factor in deciding the form of the final equipment.

The required superimposition accuracies for materials of various resolutions were determined in Section 2.1.1. If second-order corrections are necessary, there is a strong argument for using an electronic distortion removing system, where second-order corrections can be made by changing the shape of the scanning pattern. This is achieved far more easily than the corresponding correction in an optical system, where the use of tilted planes is required.

The scale of any image on a tilted photograph can be expressed as

$$S = \frac{F - y \sin t}{H - h}$$

where  $t$  = tilt angle

$y$  = distance of image from the isocenter measured in the direction of the tilt

$H$  = flying height of the camera

$h$  = ground elevation of the object

$F$  = focal length of the system used

The rate of change of scale is therefore

$$\frac{dS}{dy} = - \frac{\sin t}{H - h}$$

Tilt can also be expressed in terms of the displacement of the image (Fig. 2-4) by

$$D_t = \frac{y^2}{(F/\sin t) - y}$$

Since  $-y$  is normally small compared with  $F/\sin t$ ,

$$D_t \approx \frac{\sin t}{F} y^2$$

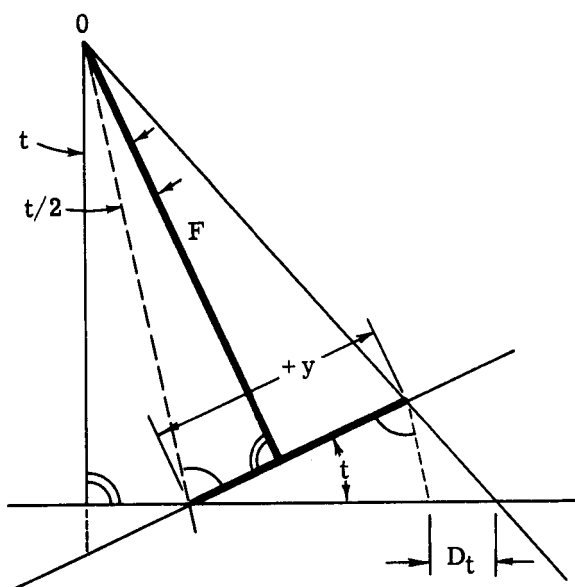


Fig. 2-4 — Image displacement due to tilt

The image displacement is therefore of a parabolic form as shown in Fig. 2-5. An automatic registration system with only first-order capability will provide a linear approximation to this curve, as shown by the line AA. The residual peak to peak error is  $2e$ . It can easily be shown that for the curve  $D = (\sin t/F) y^2$ , the residual second-order error is

$$e = \frac{\sin t}{8F} (y_2 - y_1)^2$$

where  $y_1$  and  $y_2$  define the edges of the viewed area in the  $y$  direction.

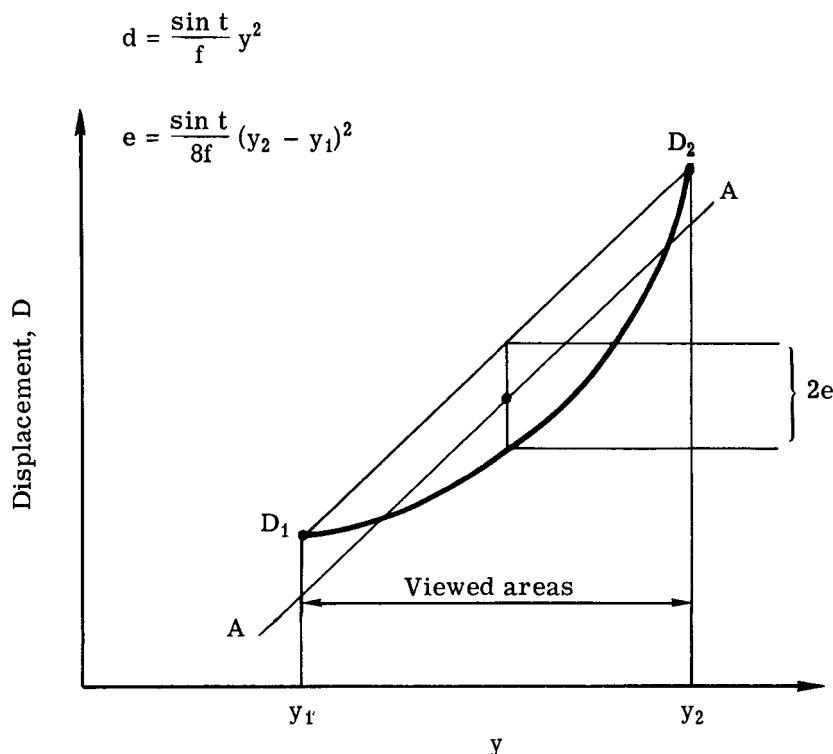


Fig. 2-5 — Residual second-order displacement error due to tilt angle

Residual second-order errors have been computed for tilt angles of 7.5, 15, 30, and 45 degrees, with camera focal lengths of 6 inches (150 millimeters), 12 inches (300 millimeters), 24 inches (600 millimeters), 48 inches (1,200 millimeters), 100 inches (2,500 millimeters), and 200 inches (5,000 millimeters). The results are shown in Figs. 2-6 through 6-11. In each of these figures, the maximum permissible superimposition errors for images of resolutions of from 25 to 200 lines per millimeter have been indicated, enabling the effect of second-order distortion on the final image to be estimated. Figs. 2-6 through 2-11 show that, in general, second-order corrections are essential, especially at large tilt angles and with high resolution imagery.

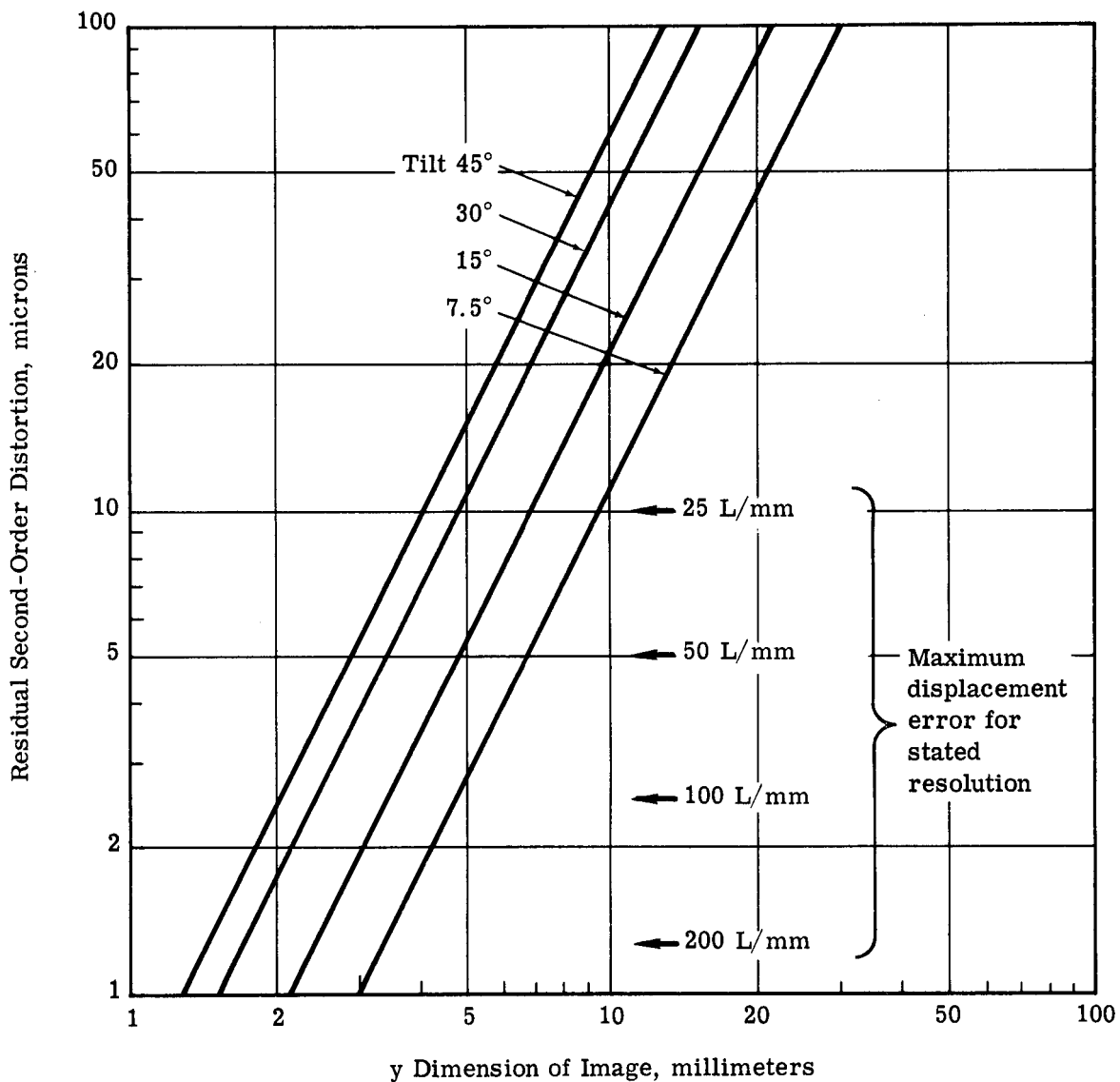


Fig. 2-6 — Residual second-order distortion for 6-inch focal length



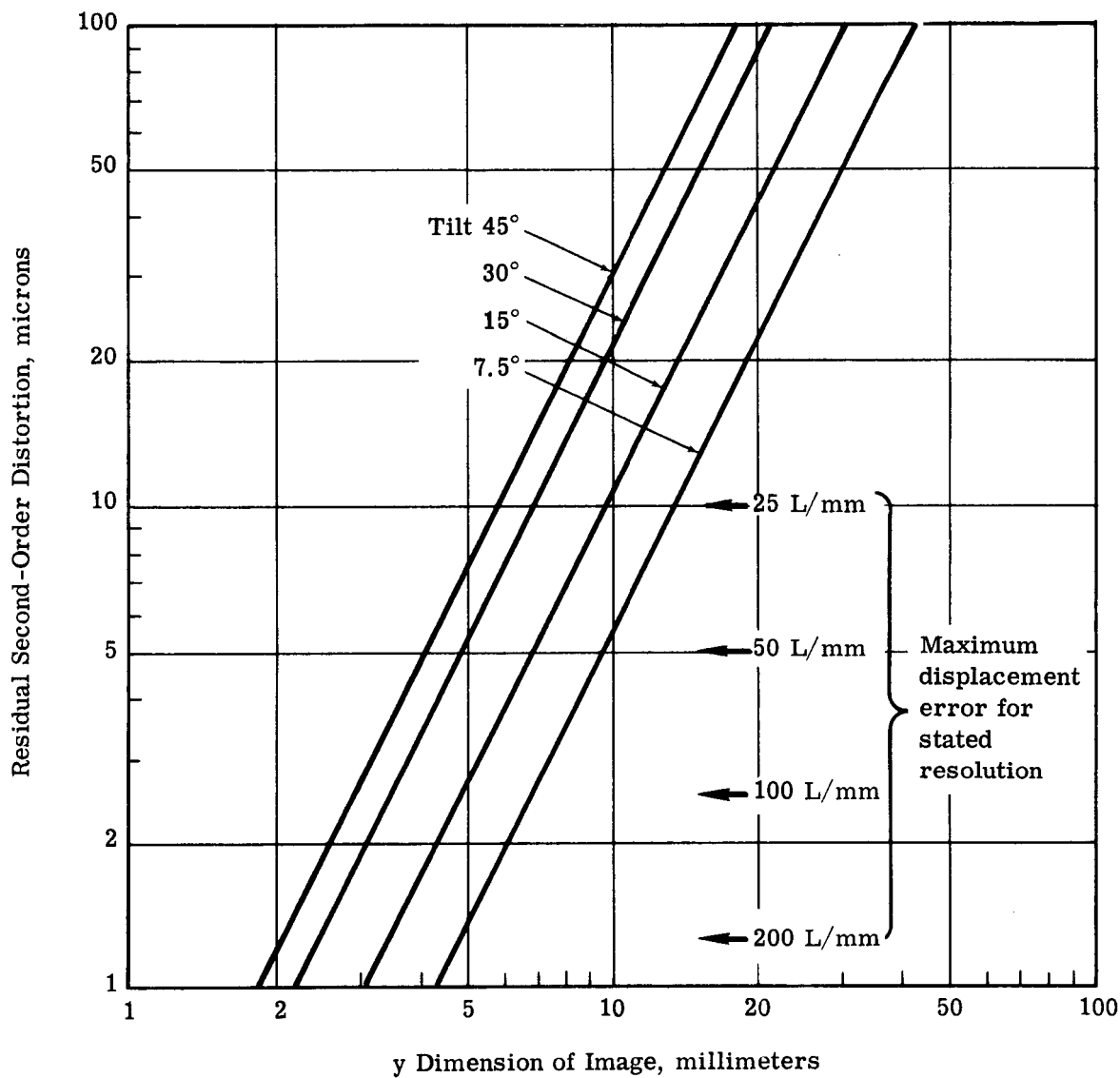


Fig. 2-7 — Residual second order distortion for 12-inch focal length

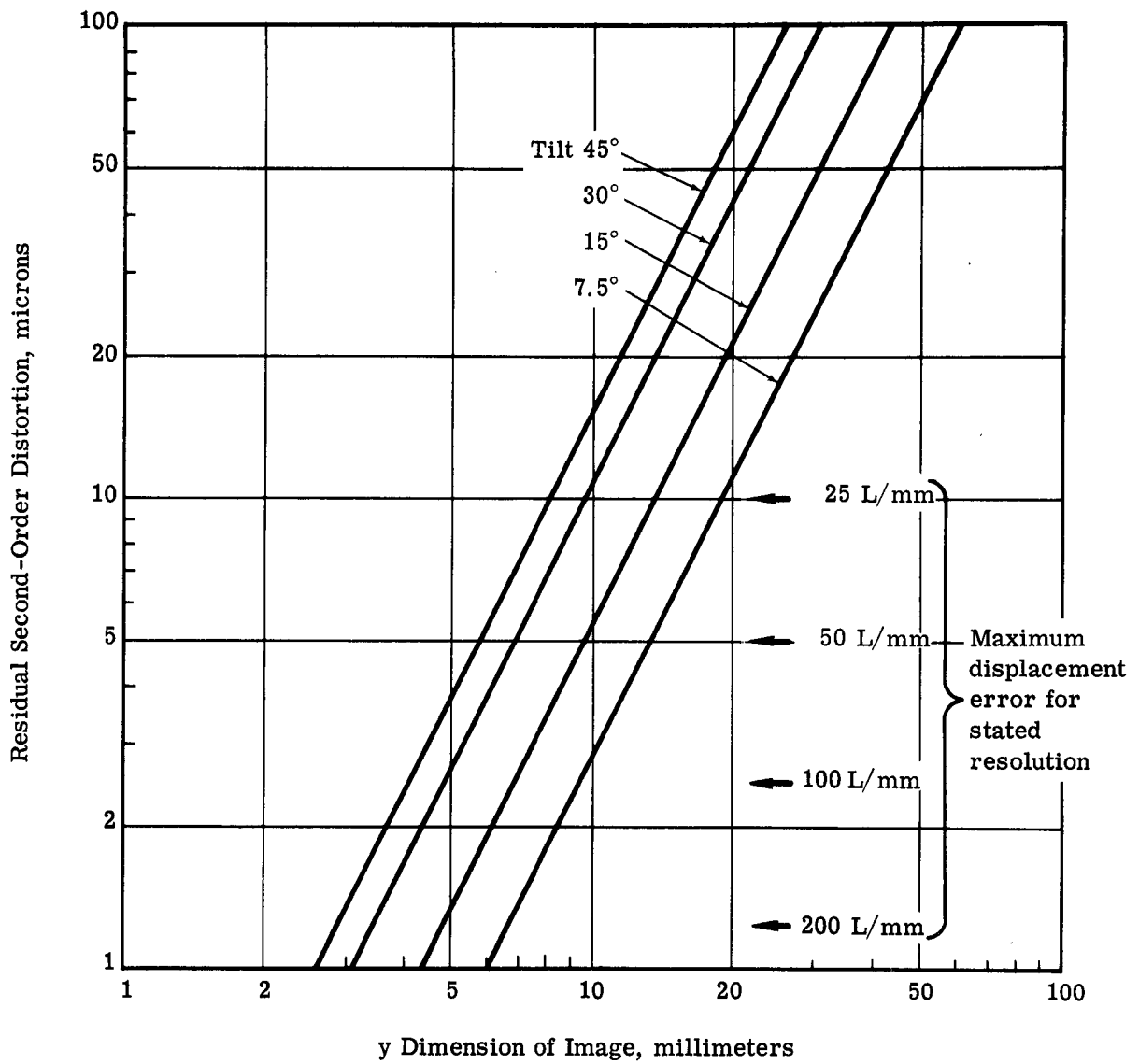


Fig. 2-8 — Residual second-order distortion for 24-inch focal length

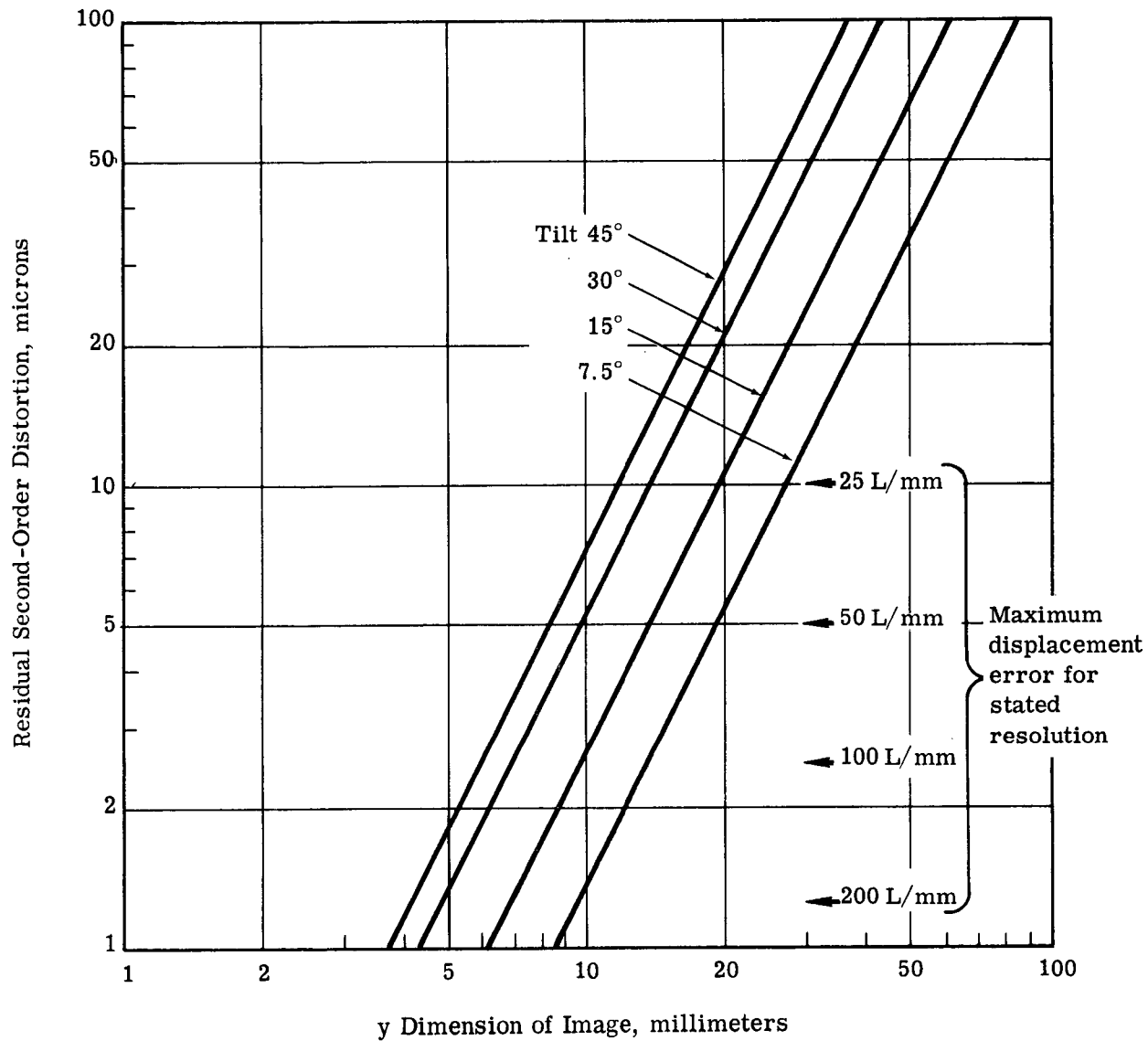


Fig. 2-9 — Residual second order distortion for 48-inch focal length

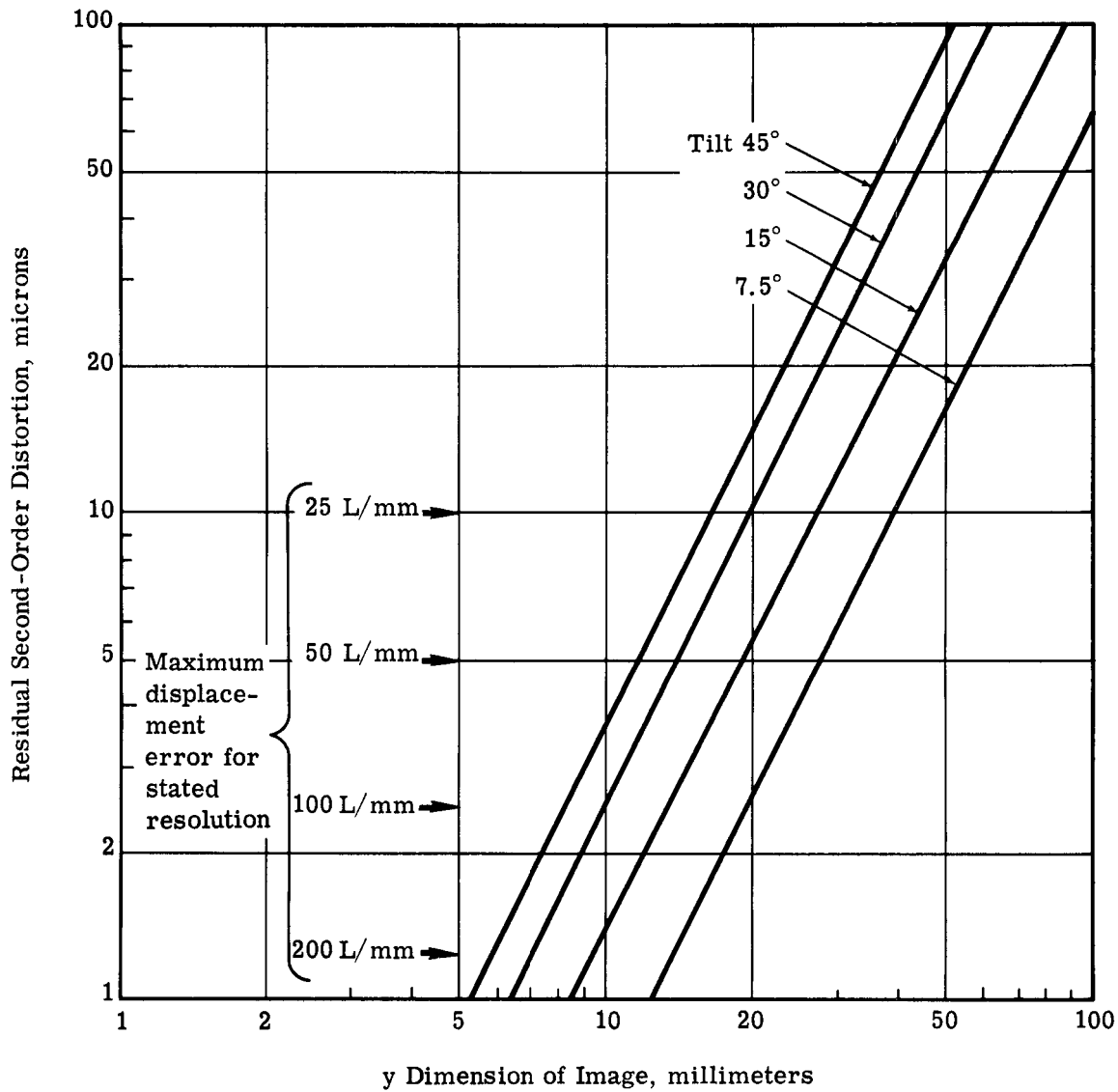


Fig. 2-10 — Residual second-order distortion for 100-inch focal length

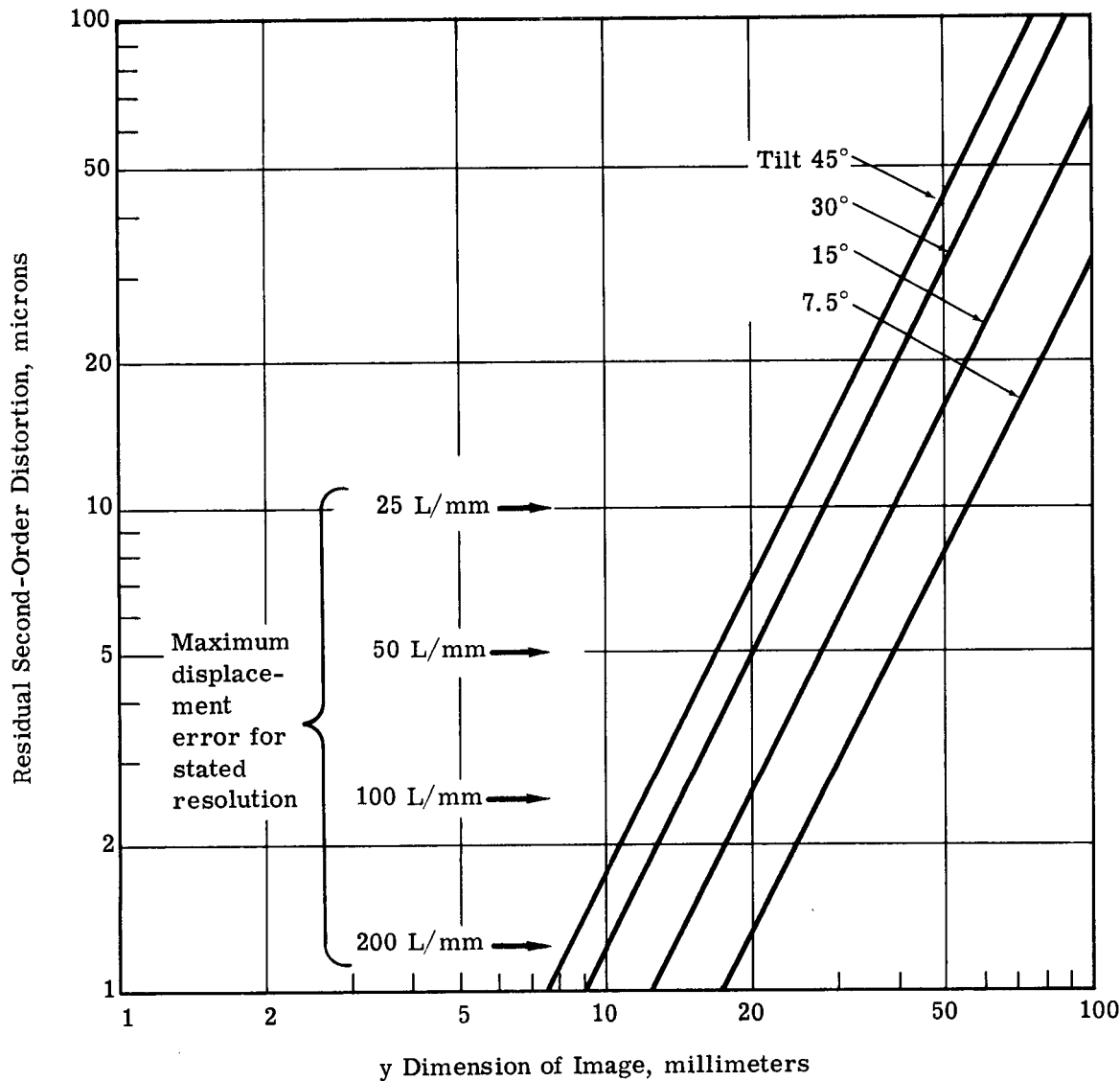


Fig. 2-11 — Residual second-order distortion for 200-inch focal length

### 2.1.3 High Order Corrections

The high order image distortion produced by relief displacement presents a problem in image integration. Obviously, the differences in imagery due to viewpoint must be eliminated or compensated for, in order to obtain the full benefits of image integration. There are two approaches to the problem (1) eliminating relief displacements by making each element of imagery congruent with the corresponding element in other inputs, and (2) using stereo viewing to take advantage of the information present in relief displacements.

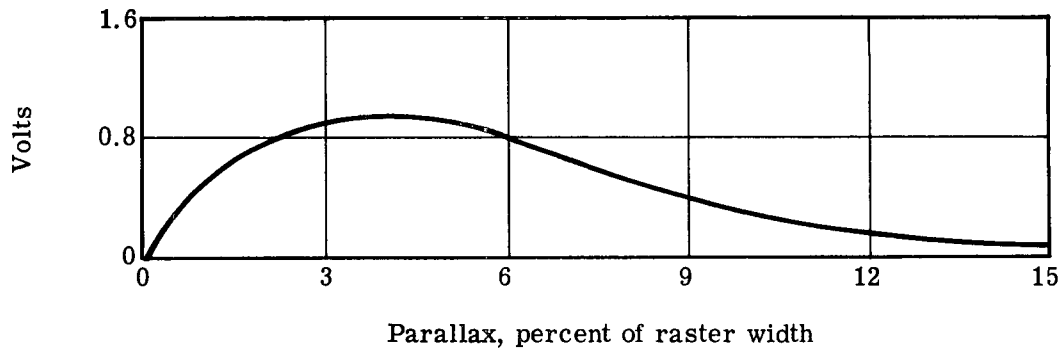
If the images to be integrated have been taken from similar viewpoints, or if the vertical relief in the viewed object is small, the problem is considerably simplified; in these cases it will be possible to directly integrate several photographs without being concerned with high order corrections. High order displacements can be eliminated on a point by point basis in an optical system, the process being similar to the production of an orthophotograph. This is, however, a slow process and not suitable for photointerpretive use. An electronic scanning system is potentially capable of removing high order image displacements almost instantaneously for direct viewing. Although this is not yet a practical reality, development of the ARES viewer to achieve this capability is being vigorously pursued at [redacted]. The best immediate solution for the integration of multiple images containing considerable vertical relief obtained from several different viewpoints appears to be to separate the input material into groups, such that the variation in viewpoint in a single group is minimized. Each group can then be integrated directly. The integrated groups can then be taken in pairs and viewed stereoscopically; each pair may involve a different stereo base line and thus give a different view of the target. This approach seems to make the best possible use of the different capabilities of a multiple image integration device and a stereo viewer. Ultimately, the development of an image integrator with high order transformation capability will enable the viewpoints to be exactly compensated, so that a single integrated photograph, or a single stereo pair, will contain all the information present in the various inputs. The proposed electronic viewer will have this add-on capability for high order image transformation, and will not become obsolescent.

### 2.1.4 ARES Correlator Performance

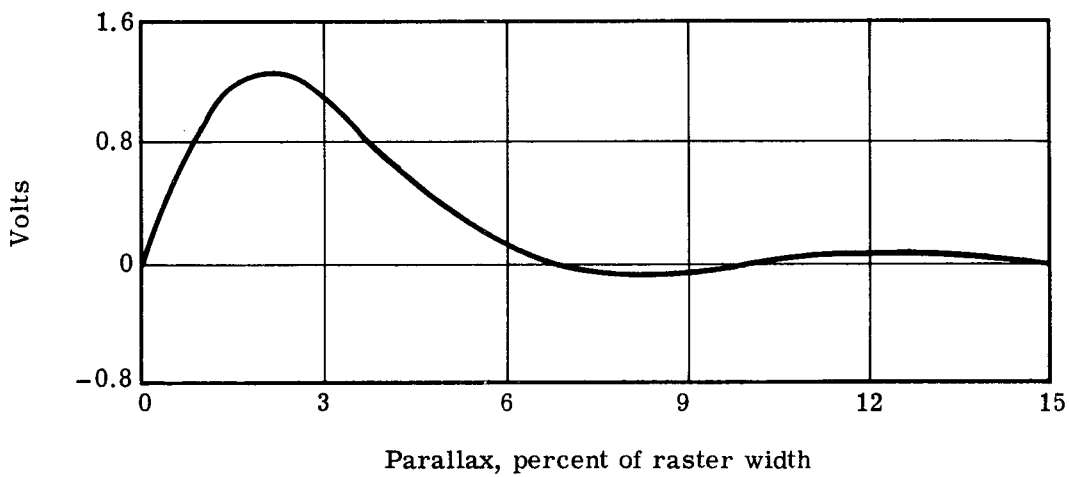
Having determined the registration accuracy requirements for image integration, we will now consider the performance of the current ARES correlator.

The ARES correlator and distortion analyzer produce their outputs by averaging the errors over the whole viewed area. The accuracy with which distortion errors are computed is not therefore limited by the number of lines in the scan, since there is a considerable integration effect present. Typical correlator transfer functions are shown in Fig. 2-12. In the process of image registration, the low frequency correlation channel comes into operation first, since this has the widest range of operation.

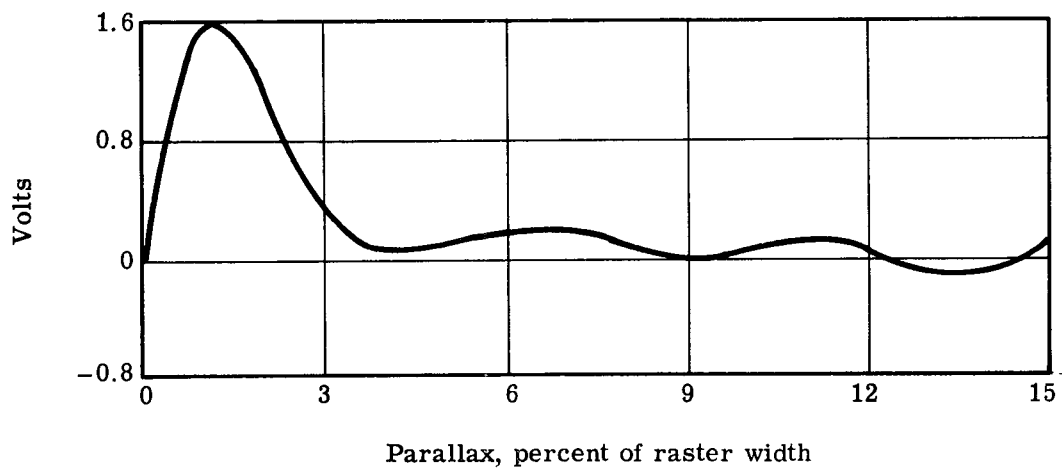
As the image parallax is reduced, the displacement comes within the range of the higher frequency channels. The lower frequency channels are successively eliminated in order to reduce their noise contribution. The final accuracy of the system therefore depends on the transfer characteristic of the highest frequency correlator channel, the loop gain of the system, and the correlator noise. The correlator transfer curve has a slope of 2 volts per 1 percent of raster width. For an image 0.25 inch square, which is the smallest viewed area in the proposed design, the correlator gain is 800 volts per inch, or 0.03 volt per micron. If sufficient loop gain is provided, the limit on registration accuracy is set by the noise level at the correlator input. The noise level varies with the type of imagery being scanned, but is of the order of 0.1 volt. The minimum displacement error that can be sensed is therefore approximately  $0.1/0.03$  or about 3 microns. This error is consistent with the displacement error that will allow a resolution of about 100 lines per millimeter in the integrated image, referred to the input material, which was determined to be 2.5 microns in Section 2.1.1 (see Table 2-1). This 3-micron displacement error corresponds to a



(a) Channel A — 100 to 215 kc/sec,  $f_c = 147$  kc/sec



(b) Channel B — 215 to 460 kc/sec,  $f_c = 316$  kc/sec



(c) Channel C — 460 to 1,000 kc/sec,  $f_c = 680$  kc/sec

Fig. 2-12 — Correlator transfer functions (raster width is 18 millimeters)

spatial frequency phase shift of 90 degrees at about 83 lines per millimeter. The amplitude of the resulting MTF of three combined images will be lower than this by a factor of approximately  $1/3^{1/2}$  or 0.58. In computing the effect of image misalignment on the final image, it must be kept in mind that an image integration viewer cannot increase the detail seen in high contrast images. The purpose of integration is to improve the signal to noise ratio, and therefore the visibility, of low contrast detail. This increase in visibility is necessarily accompanied by a small decrease in the limiting resolution of the system due to small but finite image misregistration.

## 2.2 IMAGE ENHANCEMENT

### 2.2.1 Gamma Control

Subjectively, the quality of reproduction produced by a television system is described by the term "photographic quality." The comparison between electronic display quality and photographic quality is rated in terms of the photographic system because of its higher performance. Those factors that are judged in the comparison are tonal quality, signal to noise ratio, and picture sharpness. These factors are interrelated in electronic systems, and tradeoffs are required to produce an image with satisfactory characteristics on the display system.

The control of the relationship of the reproduced gray scale to the luminance of the original subject is of importance in achieving excellent tonal quality. According to the Weber-Fechner law, the eye perceives changes in luminance in a logarithmic relationship (i.e., an increase in stimulus, dB, is proportional to the existing stimulus, B, or, for equal changes,  $\Delta B$ ,  $\Delta B/B$  is constant) therefore, the transfer function of the system is generally plotted in terms of the logarithm of the input luminance to the logarithm of the output luminance of the system.\* The gradient of the system describes the contrast of the reproduction compared to that of the original subject, and is the slope at any point of the gray scale dynamic transfer function (GTF) when plotted on log-log paper.

The maximum slope, or gradient, is termed the "gamma." A maximum slope of 45 degrees is equivalent to a gamma of 1, and indicates a 1:1 correspondence between input and output at that point. The ratio of log input to log output is thus proportional to the value of gamma.

The eye sees a uniform decrease in contrast between steps in a gray scale as the gamma is decreased below 1. However, in linear coordinates, the black end of the GTF is expanded while the highlight, or white end, is compressed. For gammas greater than 1, the opposite effect takes place, i.e., the white end of the gray scale is expanded and the black end compressed. In the latter case, the eye sees the contrast between steps increase uniformly.

Gamma is measured at the point of maximum slope and reflects the gradient maximum. Because of the nature of almost all gray scale reproducing systems, there is compression at both ends of the scale. The effect of this S distortion on reproducing systems is that for a constant GTF ratio, the gradient is increased for the central or middle grays and compressed for the highlight and shadow areas. The average gradient is therefore always less than the gamma of the system. It is the increase in overall average gradient that marks the reproduction as being inferior in quality to its original.

In photography, and particularly in the field of color reproduction, this factor is well known. Techniques such as highlight masking are used to help overcome the degradation of successive generations of reproduction.

Electronic systems are very flexible in handling this problem. Amplification of the video signal with nonlinearities inverse to those nonlinearities present in the original material and in the

---

\* Since  $d[\ln (B/B_{\max})] = dB/B$ .



video channel can correct for gray scale distortions. In fact, it is possible in some cases to improve on the original by removing tonal distortions caused by improper processing or exposure.

The basic limitation to the use of the above techniques is the noise component of the signal, whether it be derived from the original photography or generated in the video circuits used in reproducing the imagery.

The overall dynamic transfer functions of both optical and electronic systems are degraded by noise. The signal to noise ratio for an image reproducing system is a measure of the maximum to minimum contrast, or contrast ratio, that can be handled. In optical systems, the noise is caused essentially by stray or flare light which reduces the dynamic range of the system. Electronic systems suffer from this same problem of unwanted light, as well as from noise generated by the electronic components of the system.

These factors limit the amount of correction that can be supplied by electronic gamma correction. For rooting functions, as larger contrast ratios are handled, the gain ratio increases for the blacker parts of the video signal. This may involve high gains in the dark gray region, and may thereby enhance defects resulting from (1) noise generated in the transparency scanning system, (2) stray light (or flare) in lens systems, and (3) inaccurate black level adjustment.

Therefore, in correcting for the nonlinearities, as greater contrast ratios are accommodated a point is reached where the disadvantages begin to equal the advantages. This point must be determined empirically, and will vary with different inputs. Therefore, the amount of gamma correction must be controlled by the operator.

#### Gamma Correction Circuitry

In a video system, part of the characteristic is electrical, and this part of the overall GTF is expressed in terms of the ratio of the electrical input and output signals (voltage or current). A video signal which has been transferred through an ac coupling will be zero for some intermediate luminance value. When the peak to peak video signal is reduced to zero, there remains a dc component, either zero or some other value, which represents the average value of the signal. If the scene being transmitted is almost all white, the average is near the white peaks; if the scene is almost all black, the average is in the dark gray portion of the video signal.

Before the signal can be applied to a nonlinear amplifier, it is necessary to set a certain value of the signal at a fixed dc point, so that the corresponding luminance value will always appear on the nonlinear characteristic at the correct point.

Experimental work was conducted on the design of an amplifier for insertion in the ARES video channel for the correction of nonlinearities. This work was divided into three phases:

1. The establishment of a black level in the video signal by the addition of a blanking pulse to the flying spot scanner tubes
2. The development of an amplifier to drive the nonlinear circuitry and clamping system (keyed clamp), to establish an operating point at the black level during the clamping period
3. The development of a nonlinear amplifier with single knob control of the nonlinearity.

Two breadboard gamma amplifiers were constructed and installed in the ARES for evaluation. In addition, a circuit was breadboarded for electronic switching between two video inputs at various rates without flicker. The arrangement was such that it was possible to switch each of the two ARES channels to a straightthrough condition, or to insert the gamma amplifier. When inserted, the gamma amplifier output fed both the correlation channel and the video driver for the display tube.

The purpose of our tests was to demonstrate the application of manual control of gamma to enhancement of the visual display, and also to determine what effect a change in gamma would have on correlation.

Blanking signals were fed to the cathodes of the two scanning cathode-ray tubes by means of a blanking generator. The blanking signal was "folded" around the edge of the raster and its amplitude adjusted to cut off the cathode-ray tube light for 2 microseconds. The blanking pulse then appeared on the video output of the photomultiplier as a pulse representing black (absence of light), which could be used as a reference in the dc restoration circuits at the gamma amplifier and also at the grid of the viewing cathode-ray tube.

The gamma amplifier used a keyed clamp circuit to establish a constant operating point for the nonlinear amplification of the video signal. At the cathode-ray tube, it was found that the black setting circuitry of the ARES clamped this point, since it was the blackest point in the picture. It was noted that the introduction of the blanking pulse to the ARES circuitry improved the appearance of the black portions of the viewed picture, permitting observation of detail in the blacker portions that otherwise was lost due to black compression. It was also noted that the time constants of the ARES circuitry, when photographs containing large, massive areas of black were used, caused the black setting operation to take place on these areas rather than on the blanking pulse. As a result of these observations, it is recommended that keyed clamps be used at all points requiring accurate black level setting.

The circuit described above operates by detecting the blackest part of the picture and setting a constant cathode-ray beam current at this point representing black. The circuit works very well, but the results can be confusing. For example, when no photograph is in the viewing part of the ARES, the darkest part of the video signal is created by negative peaks of the phosphor grain pattern and the pattern caused by burning of the phosphor, which is a normal effect as the tube ages. The black level setter adjusted these negative peaks to represent subjective black as referred to the peak light output. The white excursions of the noise (grain and burn) signal were expanded by the automatic video gain to full peak output. Normally the grain pattern of a scanning tube phosphor has an rms value of less than 10 percent near the average signal level. However, this circuit expanded the noise signal to approximately 95 percent.

This form of image control presents the possibility of severe tonal distortion for certain types of photography, in particular, that which has no true subjective blacks. By using an established black reference point throughout the image integration viewer system, this form of tonal distortion will be avoided.

### 2.2.2 Shadow Suppression

The automatic registration of several aerial photographs of the same area taken under different conditions of illumination is sometimes difficult because of the presence of shadows or specular reflections. Shadows are a dominant feature of photographs taken with sunlight falling on the area from a low angle. Specular reflections, while less common, cause obliteration of significant detail due to saturation of the photographic material. If the shadows in the several photographs are in different positions due to a change in the position of the illumination source, or are present in only a few of the inputs, correlation is difficult to achieve. A great improvement in the operation of automatic registration circuitry can be realized if the effects of shadows can be eliminated.

A better understanding of the problem may be had from the following considerations. Assume that we have two reflection density step wedges, each of the ten steps having a density greater by 0.15 than the preceding step, with step 1 being of zero density and assumed to reflect 100 percent of the light. We place the two step wedges in the field to be photographed. At the instant we take

the photograph, a cloud obscures the illumination on one of the two tablets, reducing the illumination on it to be 8 percent of the illumination falling on the other. A second photograph is made at a later time, when the cloud has passed. Assume also that the photographic material used in making the pictures has no compression on the toe or shoulder of the density-log exposure characteristic curve.

If we then plot the density of each step on the developed photograph, our plot shows that each step when plotted against its density (Fig. 2-13) has a constant height relative to the other steps. This is how the eye sees the photograph. The step value, in terms of density, is the same whether the step is in full sunlight or in shadow.

However, when the photograph is placed in the flying spot system, the video signal will be as shown in Fig. 2-14. Since the photomultiplier of the flying spot system responds linearly, each step will be seen to decrease proportionally by a constant percentage of the previous step.

The shadowed step wedge is seen to occupy only 8 percent of the available video channel amplitude, and the brightest step is step 1. We can, by increasing the gain of the amplifier, bring shadowed step 1 up to 100 percent, or sunlight, illumination, thereby eliminating the effect of the shadow. However, if we must see some of the area outside the shadow, we cannot do this.

The other alternative is to take the logarithm of the signal shown in Fig. 2-14. On the output of the logarithmic amplifier, the steps will have equal increments and will appear as in Fig. 2-13. If, in the correlator, we differentiate the signal or pass it through a bandpass filter, thereby removing the dc component and the lower frequencies, we should be able to improve the possibilities for automatic registration.

The methods outlined above, namely (1) to look entirely within the shadow and raise the video gain, and (2) to take the logarithm of the signal and differentiate, are subject, of course, to the realities of the situation. We do not have photographic materials without compression in the toe and shoulder regions of the D-log E curve, so that even the logarithmic approach will not produce steps of equal amplitude for the shadow and highlight detail. Nevertheless, this will improve the situation and the number of photographs that can be automatically registered should be increased.

It has been our experience in the experimental application of nonlinear amplification in the correlation channel of the ARES that there is a variable in the nature of the nonlinearity that is necessary for achieving optimum conditions for automatic correlation. On certain subjects, stretching of the blacker portions of the video signal seemed to improve correlation, while for other photographs, stretching of the white was found to be more beneficial. For this reason, it is our recommendation that the operator be provided with a means of selecting the characteristic to be inserted in the correlation channel. This will be accomplished by a switch which will select one of the following functions of the video signal to be inserted in the correlation channel:

1. Square law—to emphasize the whiter portions of the signal
2. Linear—the normal mode as now used
3. Logarithmic—to emphasize the blacker portion of the signal.

### 2.3 MODULATION TRANSFER FUNCTION

The prediction of performance characteristics of both the optical and electronic systems is computed in the same manner. The response of optical and electronic systems combined can be calculated to arrive at a measure of total performance in resolution capability.

In calculating the response of the system, MTF data for each component of the system are required. Modulation transfer, sometimes called sine-wave response or contrast transmission function, relates the output amplitude of a sine-wave signal to the input amplitude as a function of

ERRATA

On p. 22 and in Fig. 2-13 and 2-14 For: 8 percent; Read: 12.5 percent

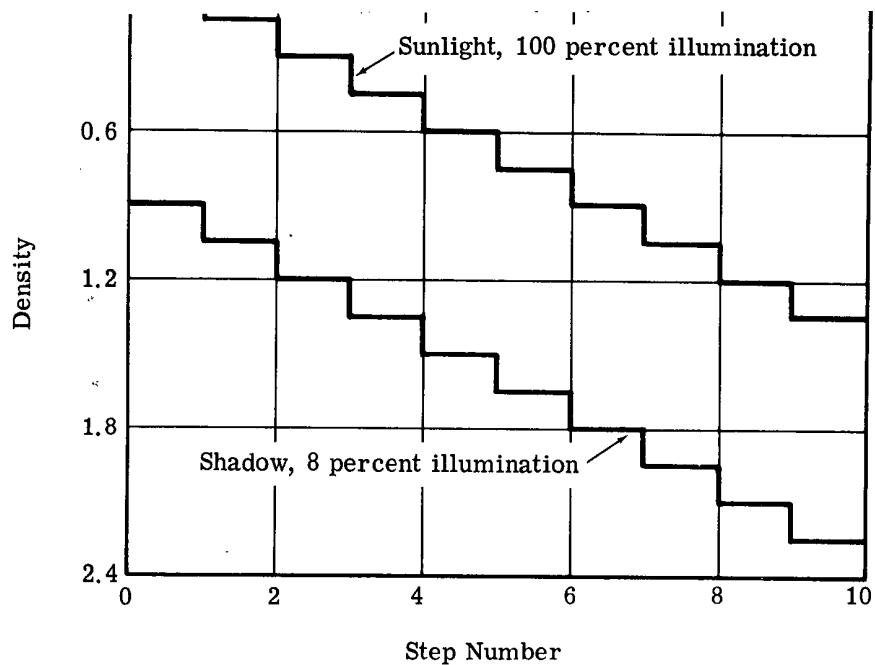


Fig. 2-13 — Log plot of step wedges in sunlight and shadow

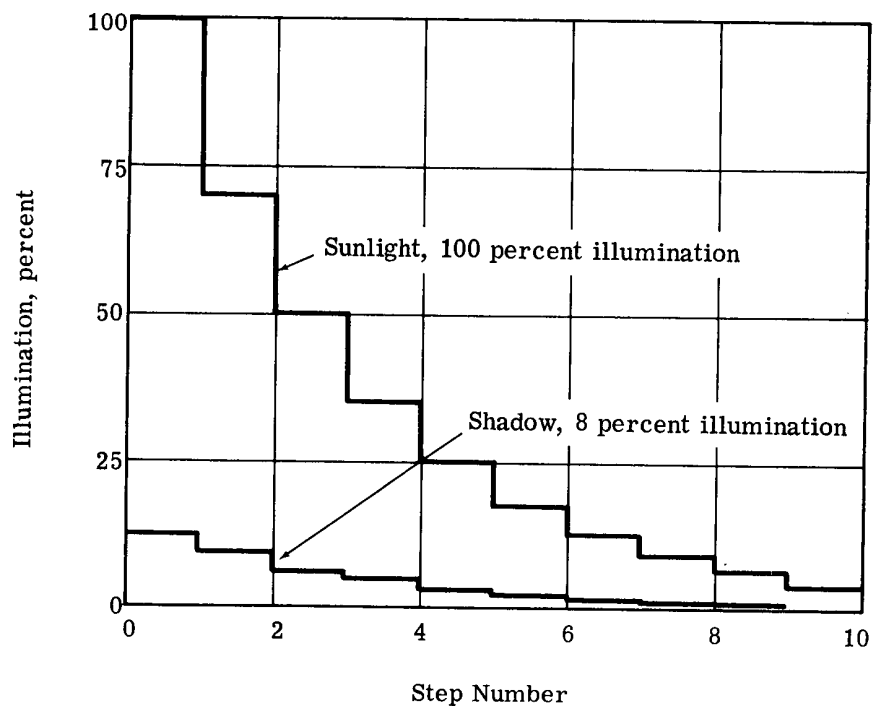


Fig. 2-14 — Linear plot of step wedges in sunlight and shadow

frequency. Simply expressed, it is the frequency response of the component or system. When the MTF of each component of a system is known, the system MTF can be obtained by finding the product of all responses for each frequency.

The term "frequency" as used in this context relates to the physical size of the picture element. The higher the frequency, the finer the size of the element. This is a crude means of expressing the differences between the concept of "spatial" or "time" domain (the former applying to optical systems, the latter to electronic or scanning systems), and "frequency" domain.

The resolution of optical systems is measured in line pairs or cycles per unit length. In electronic video systems, the number of scanning lines is fixed, and therefore, vertical resolution is also fixed. The size of the electronic display system may vary from one installation to the next. Therefore, the concept of frequency response of the video system must be related to a common factor, i.e., the height of the picture. Thus, the expression, "a 500-line picture," means that each picture element is 1/500 of the picture height, regardless of the actual dimensions of the display. Another important difference between optical and video resolution measurements is that the optical line pair is equal to two television (TV) lines. Therefore, in the display of a 3,000-TV-line picture in a raster 3 inches high, the ultimate resolution is 1,000 TV lines per inch, or 500 line pairs per inch.

It should be noted that the resolution referred to here is along the television line. The resolution in the vertical direction, i.e., at right angles to the direction of the scan line, is modified by the Kell factor. Determination of vertical resolution is a sampling process. The Kell factor states the probability that given a sine-wave test target whose frequency in TV lines is equal to the number of TV lines in the scanning pattern, and which is oriented such that each half-cycle is scanned by one TV line, (1) the output will not be zero, as would be the case if the scanning line were to traverse the test target along the zero crossing, and (2) the output will not be a maximum, as would be the case if one line traversed the peak of the positive cycle and the next the peak of the negative cycle. The actual probability is the root mean square of the two extremes, and is therefore generally considered to be equal to 0.7; hence, the average vertical resolution is 0.7 times the number of scanning lines. This means that to obtain vertical resolution equal to 3,000 horizontal TV lines, 4,200 active TV scanning lines are required. The empirical value of the Kell factor, as measured by a number of experimenters, has varied from 0.5 to 0.89, and depends on the type of display, the actual size of the video camera scanning spot, and other factors.

### 2.3.1 Flying Spot Scanning Systems

It has become the accepted procedure when generating a video signal from photographic transparencies to use a flying spot system. The system consists of a cathode-ray tube upon whose phosphor screen is generated a rapidly moving light spot, tracing out a raster by the action of an electronic beam. The light from the raster is imaged by a lens onto a photographic transparency. The light modulated by the transparency is collected by a field lens or condenser system and transmitted to a photomultiplier whose output represents the instantaneous value of transmittance of the photographic material as a function of the position of the spot in the cathode-ray tube raster. It is generally accepted that resolution and tonal qualities of the video signal generated by flying spot systems are superior to those produced by other forms of television systems, such as those which use the vidicon and the image orthicon.

The limitations of the flying spot system are imposed by the spot size of the scanning beam and the persistence of the phosphor, the latter limitation being the greater. The fastest phosphors decay to the 10 percent point in about 0.1 microsecond. This limits the practical bandwidth obtainable from flying spot systems to the order of 15 megacycles.

The requirement for a flicker-free image requires a frame rate of 30 frames per second. If, in meeting the requirements for high resolution printout, this requirement of flickerless display

can be ignored, it is possible by reducing the frame rate to transmit a larger number of picture elements within the 15-megacycle limitation imposed by the decay time of the phosphor. With a slow scan system, the persistence factor is eliminated and the limitation on resolution and contrast is imposed by the spot size and the noise generated in the photomultiplier tube.

The best combination of phosphor efficiency and phototube sensitivity is found in the P-16 phosphor, which peaks in the ultraviolet region at 370 millimicrons, in conjunction with an ultraviolet sensitive photomultiplier. This allows the best possible beam current reduction in obtaining the best signal to noise ratio. The limiting resolution of such a system for commercial television application is 800 lines per frame, with signal to noise ratios close to 100:1 (40 db).

### Image Dissector

The image dissector surpasses all known television pickup devices in resolution. All other camera tubes and flying spot scanner systems use a cathode-ray beam to perform the scanning operation or to illuminate the flying spot. The definition of a cathode-ray beam is never as sharp and exact as the direct imaging of an electronic image, as in the dissector or in an image converter tube. Measurements on an image converter with a transparent phosphor showed a resolution of 140 line pairs per millimeter (equivalent to 280 TV lines per millimeter). Comparable resolution could be achieved with an image dissector if the mechanical aperture were fine enough.\* Fig. 2-15 shows the MTF for an image dissector and a 1-mil cathode-ray tube.

The limitation on the use of the image dissector is not on obtaining sufficiently fine mechanical apertures. An aperture of 0.0003 inch in a tube will give sufficient resolution to resolve 3,000 TV lines in a 1-inch-high raster. With conventional dissector techniques at high scanning rates, this is not achievable, due to signal to noise limitations connected with the amount of photocathode illumination permitted before deleterious effects set in.

The signal to noise ratio of the dissector for a constant fixed scanning rate is proportional to the square of the linear dimension of the aperture. As a result, a dissector designed for commercial television requires an aperture of 1/500 of the picture height, or for a 1-inch raster, an aperture of 0.002 inch. Compared to a similar tube having a 1/3-mil aperture, the signal to noise ratio will be  $(2 \times 10^{-3}/3 \times 10^{-4})^2 = 4 \times 10^{-6}/9 \times 10^{-8} \approx 44$ .

The signal to noise ratio also varies as the square root of the sweep time. For a fixed photocathode loading, doubling the sweep time will increase the signal to noise ratio by 40 percent. STAT

An image dissector tube, WL-23111, manufactured by the [redacted] [redacted] has a limiting resolution of 3,200 TV lines. Its photocathode can be loaded with illumination equal to a current density of 4 microamperes. For commercial TV line scans of 63 microseconds, the tube's peak to peak signal to rms noise ratio is 0.4. This, of course, is impractical and is the reason that the image dissector has not been universally adopted for standard television systems. STAT

With conventional illumination, the WL-23111 image dissector must be used with slow rates in order to produce signals sufficiently greater than the noise component of the photocathode current. Since the signal to noise ratio varies as the square root of the scan time, a scan time of 0.6 second per horizontal line is necessary to obtain a ratio of 40:1.

For a printout system utilizing the maximum resolution of the dissector, assuming a 0.7 Kell factor, 4,200 TV lines will be required to give equal horizontal and vertical resolution and to mask line structure in the output print. The product of 4,200 lines and 0.6 second is 2,520 seconds for one frame time, or approximately 43 minutes.

\* G. Papp, On a Novel Application of the Image Dissector, J. SMPTE, 74:782 (Sept 1965).

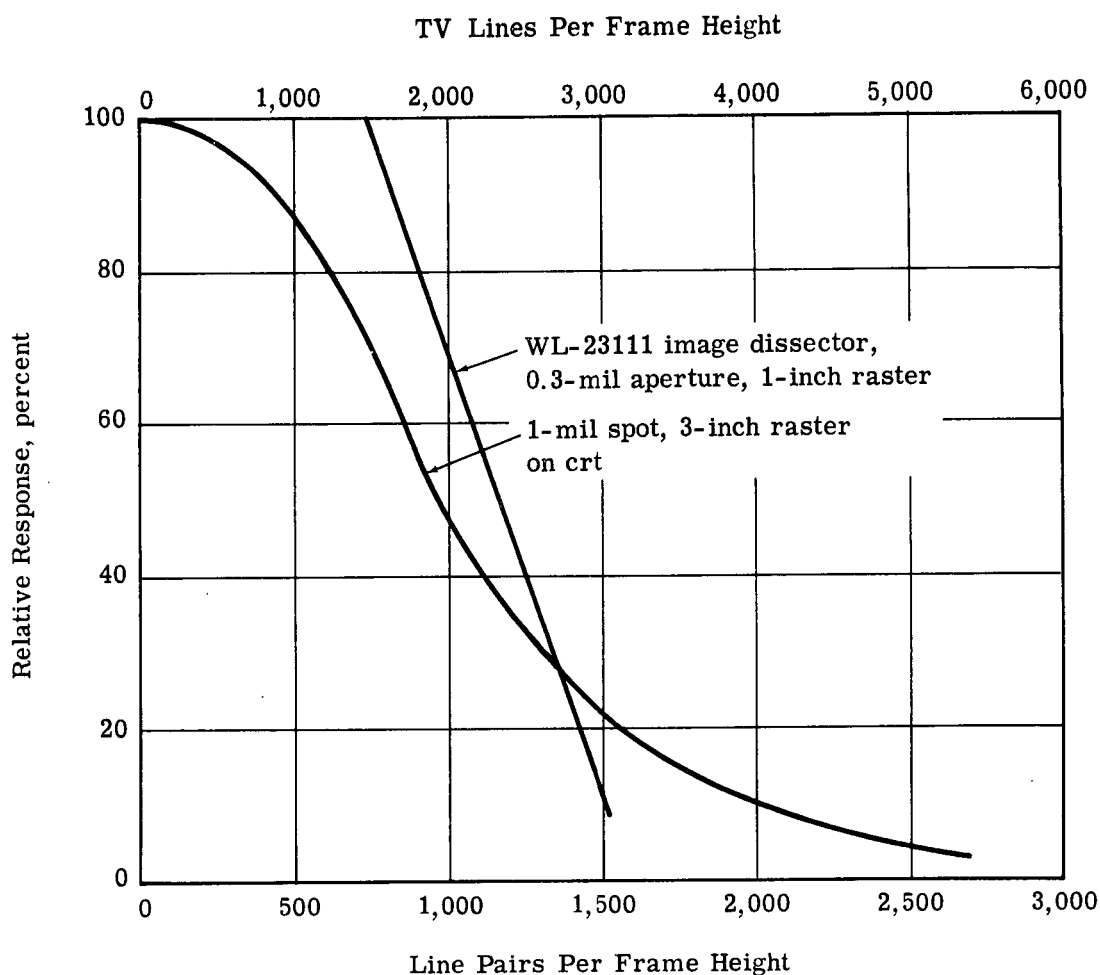


Fig. 2-15 — Modulation transfer functions for cathode-ray tube and image dissector, linear plot

#### “Follow Spot” Technique

Our discussion of the image dissector has led to the conclusion that the tube is impractical for conventional scan techniques because of the signal to noise ratio imposed by the illumination limitation. However, by using a flying spot cathode-ray tube to illuminate only the small area being directly scanned on the dissector photocathode tube, in much the manner that a “follow spot” is used in the theater to follow an actor as he moves across the stage, the signal to noise ratio of the dissector can be improved enormously. We still meet the limitation of a 4-microampere total cathode current, but because of the short duty cycle of illumination per picture element, the major portion of this current now reaches the scanning aperture.

The follow spot from the flying spot tube can be considerably larger than the picture element of the dissector tube, thereby minimizing tracking problems. The persistence of phosphor and the spot size of the cathode-ray tube do not affect the resolution of the image dissector.

This technique is currently used for high resolution displays. Its use is recommended for the image integration viewer and printout system, although the complexity of the combined image dissector and flying spot system is much greater because of the requirements for geometric scan correction and electronic zoom. However, we believe that these complexities are a small price to pay for the increased sharpness and resolution that can be obtained from the image dissector.

### 2.3.2 High Resolution Printout System

Photographic records of the superimposed imagery will be made in a module component of the image integration viewer—the hard copy printout system. The basic components of the printout station are a cathode-ray tube with high resolution display capabilities, and a P-11 phosphor imaged through a lens onto the image plane. A Graflok back will be provided at the image plane to permit the use of Polaroid materials, as well as standard 4- by 5-inch cut film and roll film.

The operation of the system will be initiated by a control on the viewer control panel, after the operator has made the necessary adjustments to the imagery as viewed on the system monitor. As discussed elsewhere, the monitor operates to provide a flicker-free display for direct viewing. When the printout operate button is depressed, the system shifts from a 30-frame operation to a slow scan mode. The linearities and geometrical transformations needed to achieve correct registration of the several inputs are stored in the system memory, which controls the scanning at each of the input stations.

#### Readout Cathode-Ray Tube

It is our objective in the design of the printout system to maintain the inherent resolution of the video signal derived from the image dissectors. To this end, the selection of the cathode-ray tube for recording the video image photographically plays an important part.

The cathode-ray tube parameters that determine its suitability for use in a photographic recording system are (1) the photoactinic light output, (2) the spot size, or ability to reproduce fine detail with good contrast, and (3) the noise or granularity of the phosphor.

The actinic light output is the result of the spectral characteristics of the phosphor, and the photographic efficiency is rated on the basis of the density obtained for a given exposure. Normally, the spectral sensitivity of the film must match the spectral sensitivity of the phosphor light output, to ensure maximum efficiency. Persistence of the phosphor is important in systems where change of information takes place in successive scans, in which case a carryover of the previous image would be detrimental. In the proposed system with a slow scan output, the persistence will improve the photoactinic efficiency. The phosphor that most closely meets the requirements for the printout system is P-11, a blue zinc sulfide. Its peak spectral output is at 460 millimicrons. Its average persistence is 60 microseconds at the 10 percent point; the actual decay time is a function of the beam current. A number of manufacturers are able to supply high resolution tubes with a fine grain version of this phosphor.

The resolution on the P-11 cathode-ray tube is dependent on the spot size formed by the electron gun on the phosphor screen. The spot dimensions are determined by the design of the electron optics of the gun and also on the amount of spreading of light that occurs in the phosphor screen material. Tubes with a nominal 1-mil spot width, measured at 60 percent of the luminance peak, are available in tubes with a 4 1/2-inch optical quality screen. A raster 3 inches square will fit within this circle. If the spot shape is to be Gaussian, its transform to frequency response is also Gaussian, as expressed by

$$F = \exp(-2\pi^2 f^2 \sigma^2)$$

where F is the percent modulation for a spatial frequency, f, and the spot width measured at 60 percent of peak output is  $2\sigma$ .

The results of a computation using this relationship are plotted in Fig. 2-16 for a raster of 3-inch frame height, and a Gaussian spot width of 1 mil. The 3-inch raster and 1-mil spot size are compatible with the 4,200 active line scan proposed for printout. The frequency response of the WL-23111 image dissector is plotted in terms of its frame height, and the combined result of



the dissector and the output cathode-ray tube is computed and plotted. It is seen that the 50 percent response point for the two is approximately 850 line pairs per frame height. The limiting response (3 percent) is approximately 1,400 line pairs.

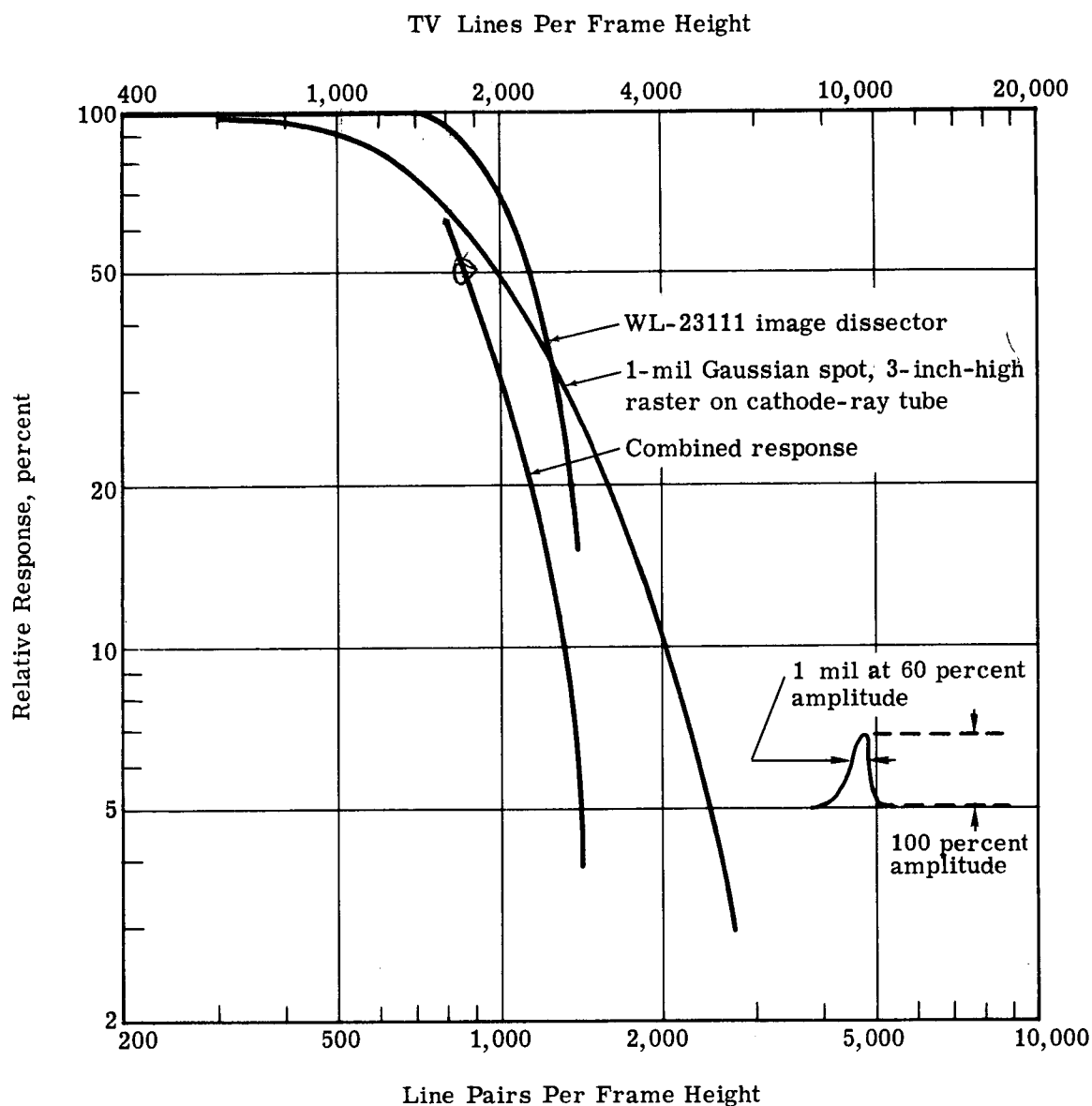


Fig. 2-16 — Modulation transfer functions for cathode-ray tube and image dissector, logarithmic plot

The magnification required for printout is dictated by the film size, usually 4 by 5 inches, or if roll film is used,  $2\frac{1}{2}$  by  $3\frac{1}{2}$  inches on 70-millimeter film. It is recommended that the output device operate at a 1:1 magnification for all film sizes.

For 1:1 magnification, 850 line pairs in 3 inches corresponds to 12 lines per millimeter on the film plane. The MTF for the film and imaging lens show almost full response at this point; thus, the film image should have essentially the same response as appears on the face of the cathode-ray tube.

Twelve lines per millimeter is somewhat finer detail than the eye can resolve at a 10-inch viewing distance. A magnification of  $2\times$  will bring the finest detail within the resolving capability of most observers.

It should be recalled that we have not been discussing the limiting resolution of the system as is normally done in optical and photographic systems, but rather the 3 db down or 50 percent response point. This is compatible with measurements made on electronic equipment.

#### 2.4 COMPARISON OF ELECTRONIC AND OPTICAL IMAGE INTEGRATION SYSTEMS

A comparison of the features of electronic and optical image integration systems is given in Table 2-2. The features examined are those essential to an integration viewer, i.e., sensing of parallax, transformation capability for handling inputs of varying geometry, gray scale processing, resolution, and type of output.

This is not intended as a general comparison between electronic and optical viewers. In a scanning viewer, for example, the resolution of an electronic system would be restricted by the necessity of presenting the information at a high frame rate. A high frame rate is not required in an integration viewer, since the imagery is essentially static.

In summary, it can be stated that for the present purpose an electronic system has the advantage of a far greater flexibility in image transformation and gray scale processing. The limiting resolution of the hard copy image on film based on a crt spot size of 1.5 mils would correspond to about 100 lines per millimeter over an area of 6 by 6 millimeters at the input film. The total number of image elements is about  $1.6 \times 10^6$ . Maximum overall magnification will be  $12\times$ , giving an output image area of 3 by 3 inches, with a limiting resolution of about 8 lines per millimeter.

An optical image integration system would be limited as to the types of materials that could be handled, as regards image geometry and film processing (e.g., negative material could not be mixed with positive). Our experience with the EROS stereo viewer indicates that the limiting resolution of the final image in an optical viewer using anamorphic and zoom lenses corresponds to about 150 lines per millimeter in the center and 50 lines per millimeter at the edge of a field about 8 millimeters in diameter, referred to the input material. This represents about  $2 \times 10^6$  image elements, which does not differ greatly from the capacity of the electronic system.

Table 2-2 — Comparison of Electronic and Optical Image Integration Systems

Feature	Electronic System		Optical System	
	Available	Remarks	Available	Remarks
Sensing of parallax	Yes	Electronic scanning	No	Possible future use of coherent light
Transformation capability				
Zero order	Yes	Move scanning raster	Yes	Move input
First order	Yes	Distort scanning raster	Yes	Anamorphic lenses
Second order	Yes	Distort scanning raster	Yes	Tilted plane
Higher orders	Yes	Distort scanning raster	No	—
Gray scale processing				
Negative-positive polarity inversion	Yes	Invert video signal	No	Reflection method not suitable for transparencies
Contrast	Yes	Change video gain	Yes	Limited, change coherence of illumination
Nonlinear characteristic	Yes	Change video characteristic	No	—
Edge enhancement	Yes	High pass filter	Yes	Spatial filter
Shadow suppression	Yes	Logarithmic amplifier and high pass filter	No	—
Noise suppression	Yes	Low pass filter	Yes	Spatial filter
High resolution				
Static imagery	Yes	$1.6 \times 10^6$ image elements	Yes	$2 \times 10^6$ image elements
Changing imagery	No	Limited by bandwidth of image transducers	Yes	$2 \times 10^6$ image elements
System output				
Direct viewing	Yes	Long persistence crt	Yes	Aerial image or screen
Hard copy output	Yes	CRT film recorder, high resolution	Yes	Film
Remote viewing-printing	Yes	Remote crt	No	—

### 3. GENERAL DESCRIPTION OF MULTIPLE IMAGE INTEGRATION VIEWER-PRINTER

This section describes the present design of the multiple image integration viewer-printer, with regard to producing this unit as deliverable hardware. Certain detailed design remains to be completed in certain areas, and will be finished during the development effort.

The general configuration of the multiple image integration viewer-printer is shown in Fig. 3-1, and a block diagram of the unit is shown in Fig. 3-2. The unit is housed in a console 78.5 inches in length, 69 inches in height, and 47 inches in depth. A viewing table projects from the front of the console, and is 38 inches above the floor. Casters are attached to the console for ease of movement, and access panels are provided to facilitate equipment adjustment and maintenance. The three separate input channels within the console each have a hinged control panel located on the front of the console. The input platens for each channel are located on the viewing table. Display units provided are the viewing monitor and the 5-inch cathode-ray printout tube. A 4- by 5-inch camera can be attached to the face of the printout tube to provide a hard copy record.

#### 3.1 CONTROL PANEL

The control panel of the multiple image integration viewer-printer is shown in Fig. 3-3. The function of each control is as follows:

- FILM DRIVE—drives the film forward, backward, left, or right
- ZOOM—selects magnifications of 0.925 $\times$ , 1.66 $\times$ , or 3 $\times$
- GAIN—varies the intensity of the video signal
- FLICKER—selects the flicker frequency, and switches the video on and off
- GAMMA—adjusts the shape of the video gain curve
- CORRELATION WEIGHTING—selects the square root, linear, or log function
- POSITIVE/NEGATIVE—selects the positive or negative video signal
- X in X—linear x-scale adjustment
- Y in X—y-skew adjustment
- X<sup>2</sup> in X—oblique scale adjustment
- XY in X—keystone adjustment
- X in Y—x-skew adjustment
- Y in Y—linear y-scale adjustment
- X<sup>2</sup> in Y—oblique scale adjustment
- XY in Y—keystone adjustment

#### 3.2 INPUT PLATEN

The configuration of the three input platens is shown in Fig. 3-4. The three input platens are located on the glass tabletop (1/4-inch-thick, "Parallel-O-plate" glass), which is illuminated

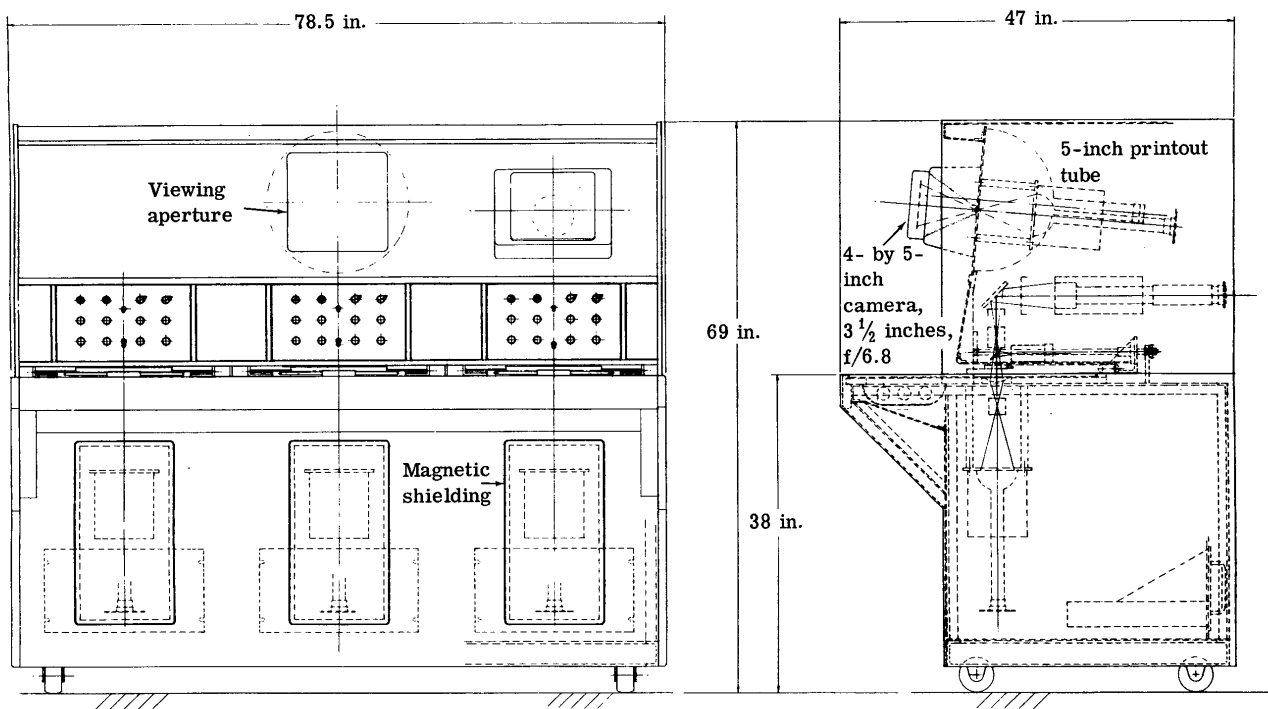


Fig. 3-1 — General configuration of multiple image integration viewer-printer

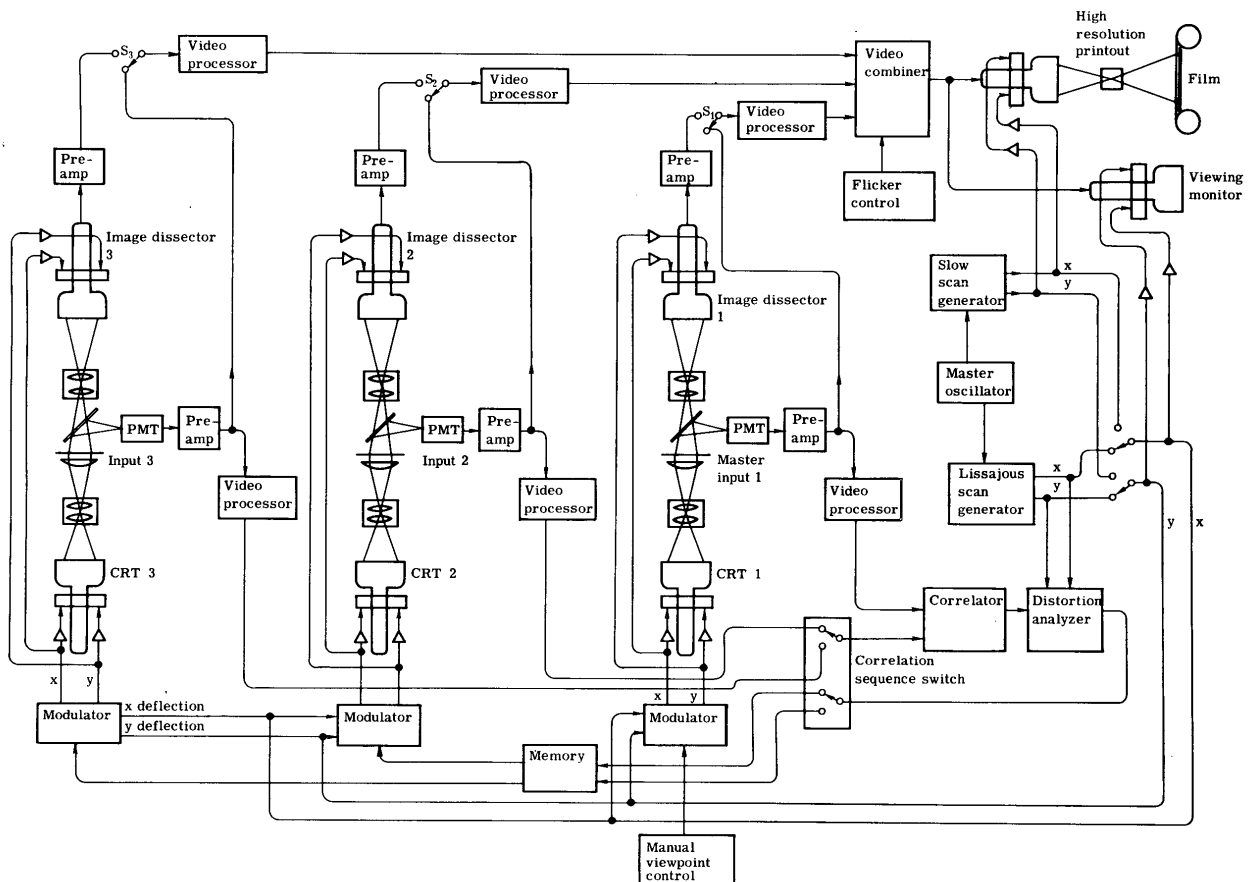


Fig. 3-2 — Block diagram of multiple image integration viewer-printer

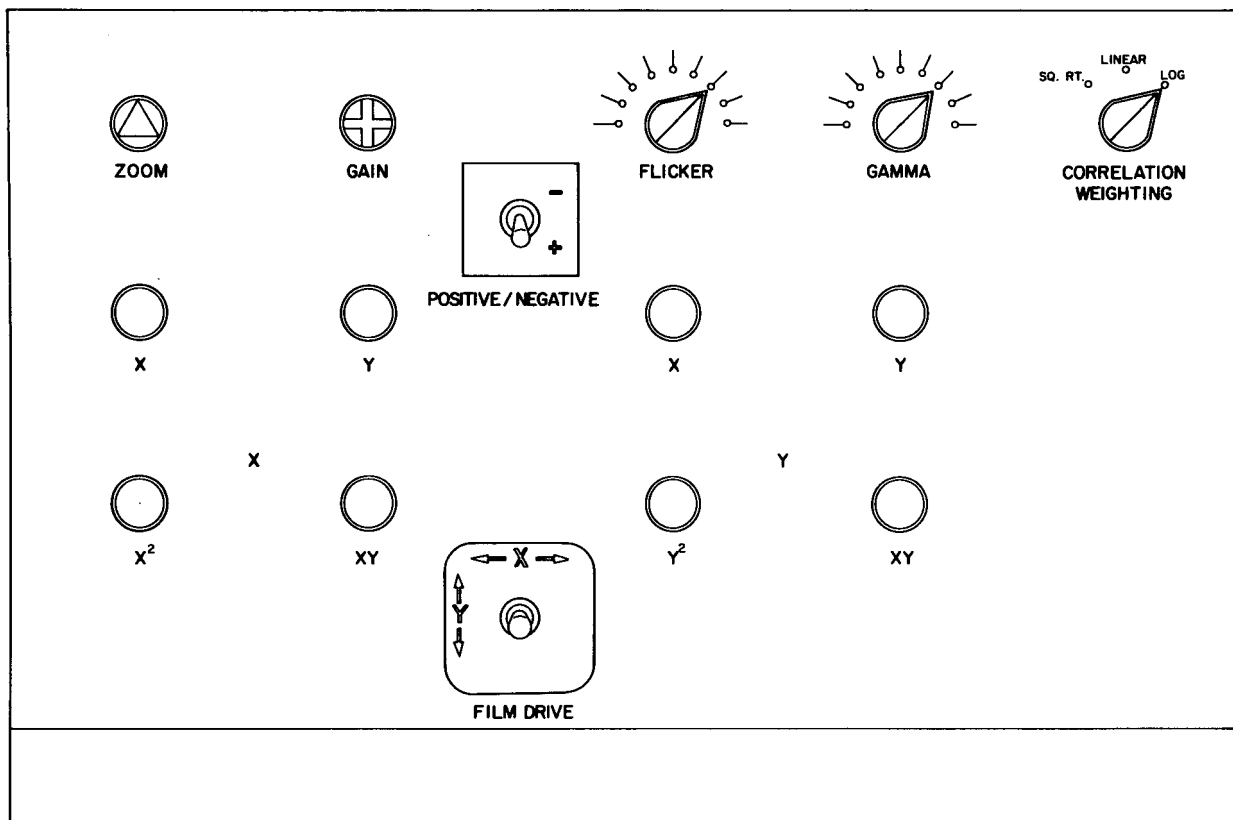


Fig. 3-3 — Control panel

from below to allow viewing and positioning. Since the distance from the emulsion plane to the lens must be within 0.002 inch for an  $f/2$  system, close tolerance control of the platen will be accomplished by supporting the glass tabletop on an air inflated rubber sheet, which will support the glass plate evenly over the entire area. The height of the rubber sheet will be controlled by three self-aligning exhaust valves which can be adjusted to provide a definite positioning of the sheet, and consequently, the glass plate.

The platen can accommodate 9- by 9-inch and 70-millimeter film chips, which are placed between two pieces of glass. The platen is translated in both the x and y directions by the joystick control, through the use of ball screws and a motor-clutch arrangement. Disengagement of the clutches allows manual positioning of the platen.

The section of film to be scanned is placed on the index registration mark, and when the platen is actuated, the desired area of film will move under the scanning tube. Manual positioning can be accomplished by handcranking or by positioning the platen by hand. The platen rests on three air bearings that are operative during platen positioning to provide smooth movement.

### 3.3 OPTICAL SYSTEM

The optical system (Fig. 3-5) performs the following three functions:

1. Images the light from the flying spot scanner onto the film
2. Collects the light passing through the film and sends it to a photomultiplier tube
3. Images the film onto an image dissector tube.

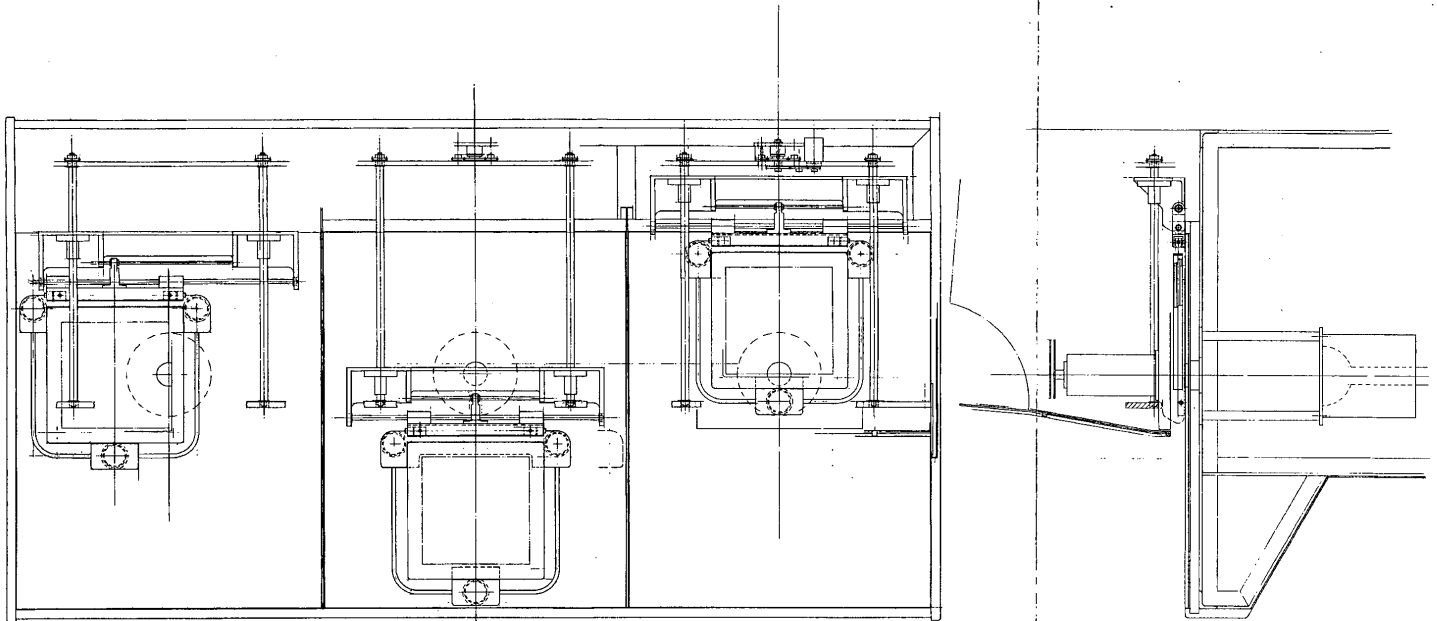


Fig. 3-4 - Configuration of input platens



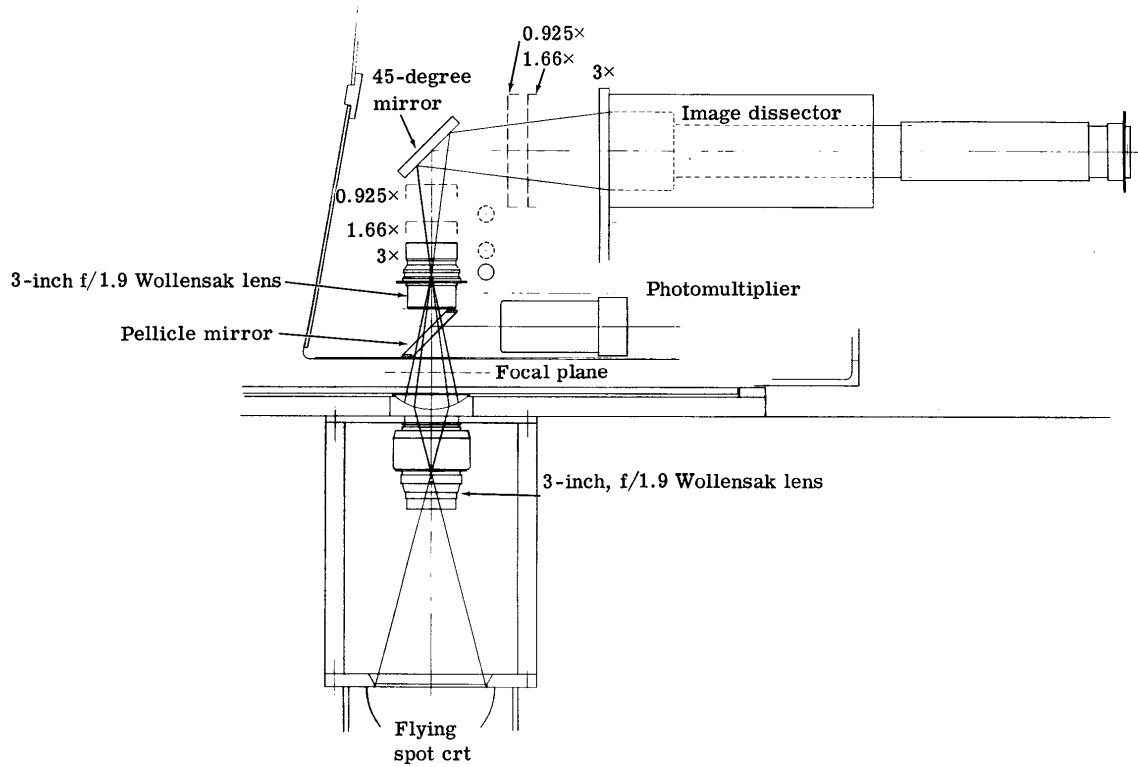


Fig. 3-5 — Diagram of optical system

Functions 1 and 2 are used in driving the correlation circuitry, while function 3 is used to obtain the high resolution video information. Function 1 provides the light source for function 3 by scanning the image dissector synchronously with the flying spot scanner.

Function 1 is accomplished with a lens designed for a P-11 phosphor spectral output, and corrected for the 2:1 conjugate ratio. The lens will be a 75-millimeter-focal-length, f/1.9, Wollensak Oscillo-Raptar. It will perform adequately at full aperture, although it may be stopped down to f/2.8 to improve the depth of focus.

The phototube pickup lens for function 2 will be located below the film so as to be out of the high resolution portion of the optical path. It will be a simple planoconvex lens with a 1-inch diameter and 2-inch focal length. The pickup lens will image the 75-millimeter lens aperture onto the front face of the photomultiplier tube. A beam splitting pellicle mirror will be used to deviate this beam onto the phototube. This pellicle mirror is manufactured by the National Photocolor Company, and is used to avoid having a tilted, thick glass plate in the high resolution system. The pellicle mirror also avoids ghost images from the back surface.

The high resolution system uses another 3-inch Oscillo-Raptar lens. This system would ideally move the lens through a range of distances to give a continuous zoom capability, but this is difficult to accomplish because of the need to dynamically maintain focus. For the purpose of this equipment, it will be adequate to provide three discrete magnifications and to zoom the raster size on the image dissector to fill in the gaps.

The lens magnifications chosen are 0.925 $\times$ , 1.66 $\times$ , and 3 $\times$ . The lens performance, referred to the film plane, will be better than 100 lines per millimeter at all points in the field, at all magnifications. At the highest (3 $\times$ ) magnification the resolution will be better than 150 lines per millimeter.

### 3.4 CORRELATION SYSTEM

The correlation subsystem consists of the following components:

1. Lissajous scan generator
2. Photomultiplier tubes and video amplifiers
3. Video correlator and distortion analyzer
4. Memory unit
5. Modulator.

#### 3.4.1 Lissajous Scan Generator

To detect image parallax, a scanning pattern must be used in which motion of the scanning spot has components in both the x and y directions. The crossed diagonal, or Lissajous, pattern formed by two triangular waveforms of slightly different frequencies has been found to be ideal for this purpose. Each point on the image is scanned successively in four orthogonal directions, enabling image parallax in any direction to be computed.

A scanning pattern using 500 lines across the diagonal will be used for this equipment, with a line frequency of 15 kc/sec and a frame rate of 30 cps. A diagram of the Lissajous scan generator is shown in Fig. 3-6. The x and y frequencies are derived through binary dividers from a common master oscillator, which ensures a fixed phase relationship between the frequencies. This is necessary in generating a stable pattern. In addition to the x and y deflection signals, this unit also provides the x and y reference signals that are required in the distortion analyzer. The 0- and 90-degree reference signals at 15 kc/sec are produced by further dividing the normal and inverted 30-kc/sec signals at the output of the main divider by a factor of two. This ensures an accurate phase difference.

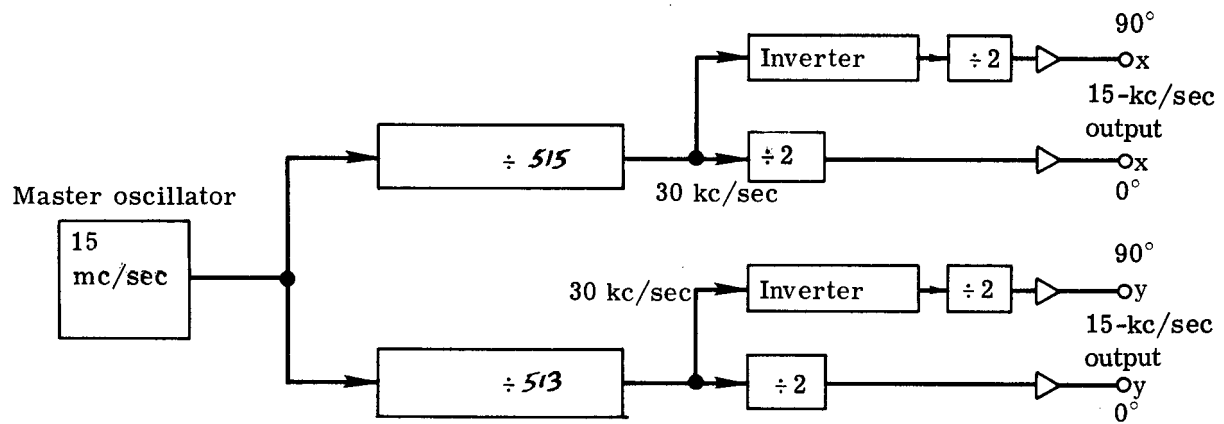


Fig. 3-6 — Lissajous scan generator

### 3.4.2 Photomultiplier Tubes and Video Amplifiers

The photomultiplier tubes pick up the fluctuating light intensity produced by density variations in the film as it is scanned by the flying spot, and convert it into a varying electric current. This current is then amplified by the video preamplifier and applied to the video processor. The video processor has provisions for polarity change to accommodate both positive and negative input material, gain control to account for differences in image contrast, and gamma control, so that the shape of the video input and output characteristics can be changed to suit the input material.

### 3.4.3 Video Correlator and Distortion Analyzer

The video signals are correlated by separating the video into three frequency bands, each channel covering about one octave. One channel of the video correlator and distortion analyzer is shown in Fig. 3-7. After band filtering, the left and right inputs are phase shifted by +45 degrees and -45 degrees, and hard limited so that only the zero crossings are preserved. The two signals are then applied to an exclusive OR circuit. The output of this unit, when the inputs are identical, consists of a symmetrical square wave. When either positive or negative phase shifts are present between the video inputs, indicating parallax between the images, the symmetry of the square wave is shifted to either positive or negative.

The output of the video correlator is applied to the analyzer modules. Parallax in the x and y directions is detected by multiplying the video correlator output by the x and y reference signals, delayed by suitable amounts to equalize the delay of the video processor and correlator. The x parallax and y parallax signals are further multiplied by the x and y 90-degree reference signals to detect the first-order distortion errors, i.e., x scale, x skew, y scale, and y skew.

The correlator and analyzer modules are mounted on printed circuit boards and extensive use is made of solid state integrated circuit components.

### 3.4.4 Memory Unit

The memory unit (Fig. 3-8) stores the error signals from the distortion analyzer in the form of the voltage to which a potentiometer is set. Six potentiometers per channel are required to store the zero- and first-order error signals. The potentiometers are servo driven so that the voltage at the potentiometer wiper equalizes that of the error input. The correlation sequence switch initiates operation of each channel, in turn, by activating the servoamplifier. When the potentiometer has been driven to equalize the error voltage, the null at the output of the differential amplifier is detected; when all channels have been nulled, the sequence control switches to the next channel.

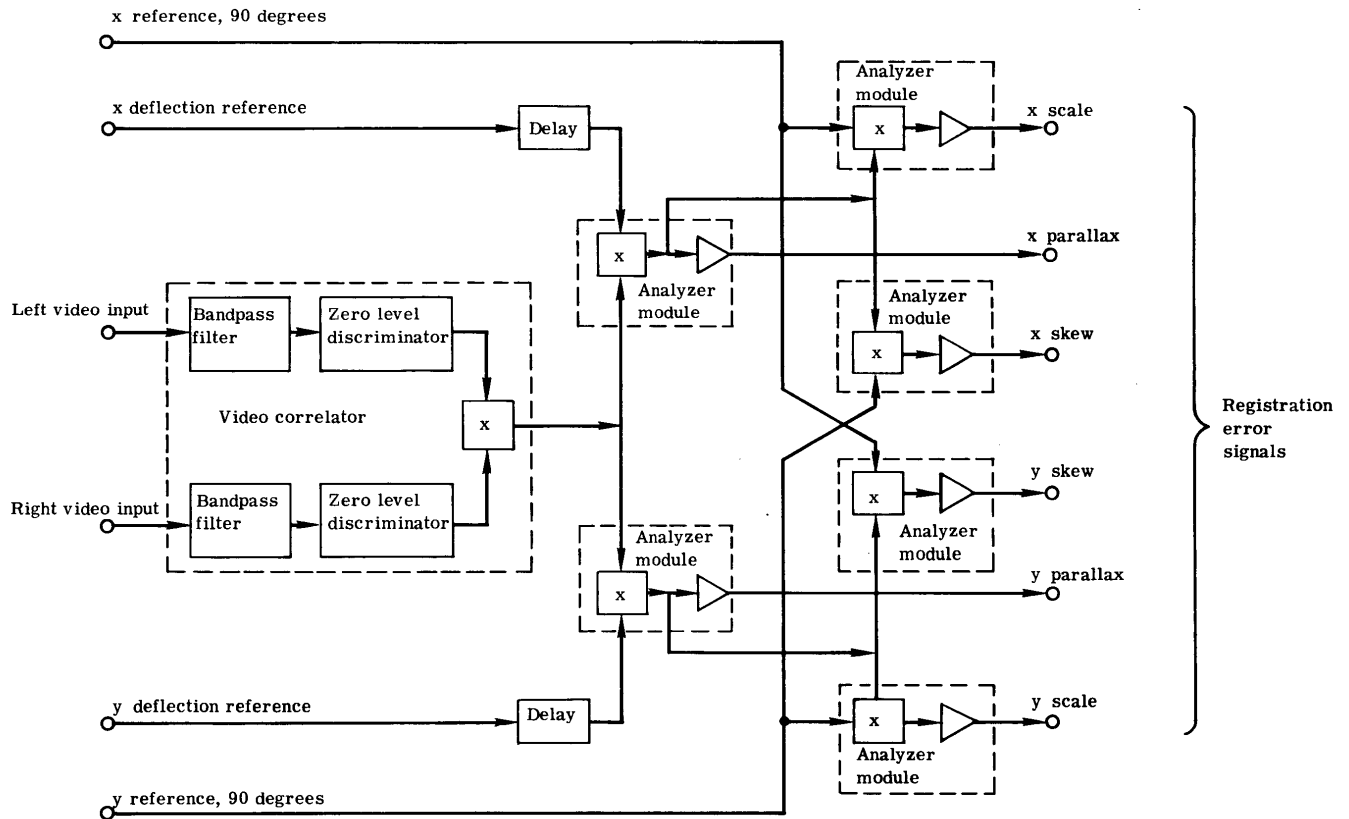


Fig. 3-7 — One channel of video correlator and distortion analyzer

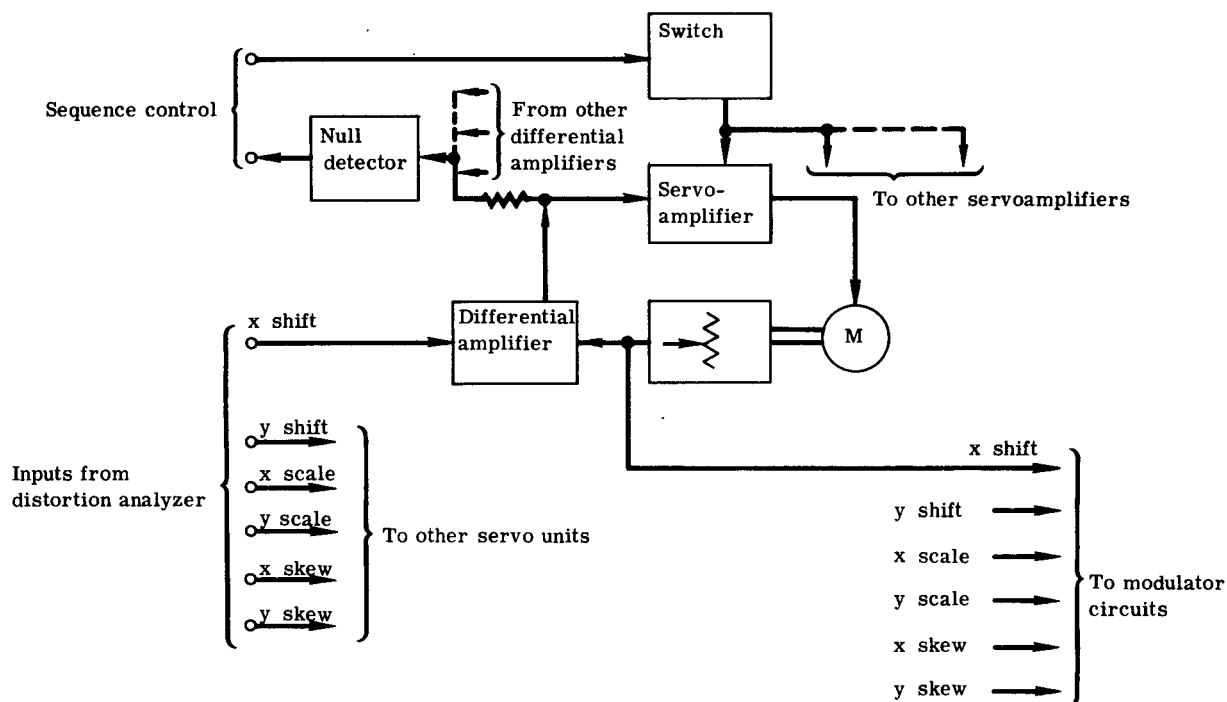


Fig. 3-8 — Block diagram of memory unit

### 3.4.5 Modulator

The function of the modulator is to distort the scanning pattern applied to the cathode-ray tubes and image dissectors in accordance with the error signals stored in the memory unit. The modulator unit shown in Fig. 3-9 consists essentially of several linear balanced modulators and summing circuits.

The x and y scanning waveform inputs are controlled by the positive or negative error input voltages, and are added to the main x and y scanning waveforms. For example, to compensate for a positive x scale error, a certain proportion of the x scan waveform is added to the basic x deflection, resulting in an increase in the x scanning amplitude. Similarly, an x skew error is compensated for by adding a certain proportion of the y scan waveform to the basic x deflection.

The modulator units are mounted on printed circuit boards and make use of integrated solid state circuitry.

## 3.5 VIDEO PROCESSING

### 3.5.1 Video Processor

The output of the image dissector is fed to a preamplifier and polarity selector that permits selection of either positive or negative display. The output of the polarity selector is fed to the video processor. Fig. 3-10 is a block diagram of one of the three image dissector channels of the multiple image integration viewer-printer.

The camera preamplifier is essentially an impedance transforming stage whose output is at a level that enables it to drive a low impedance line terminated at the video processing unit.

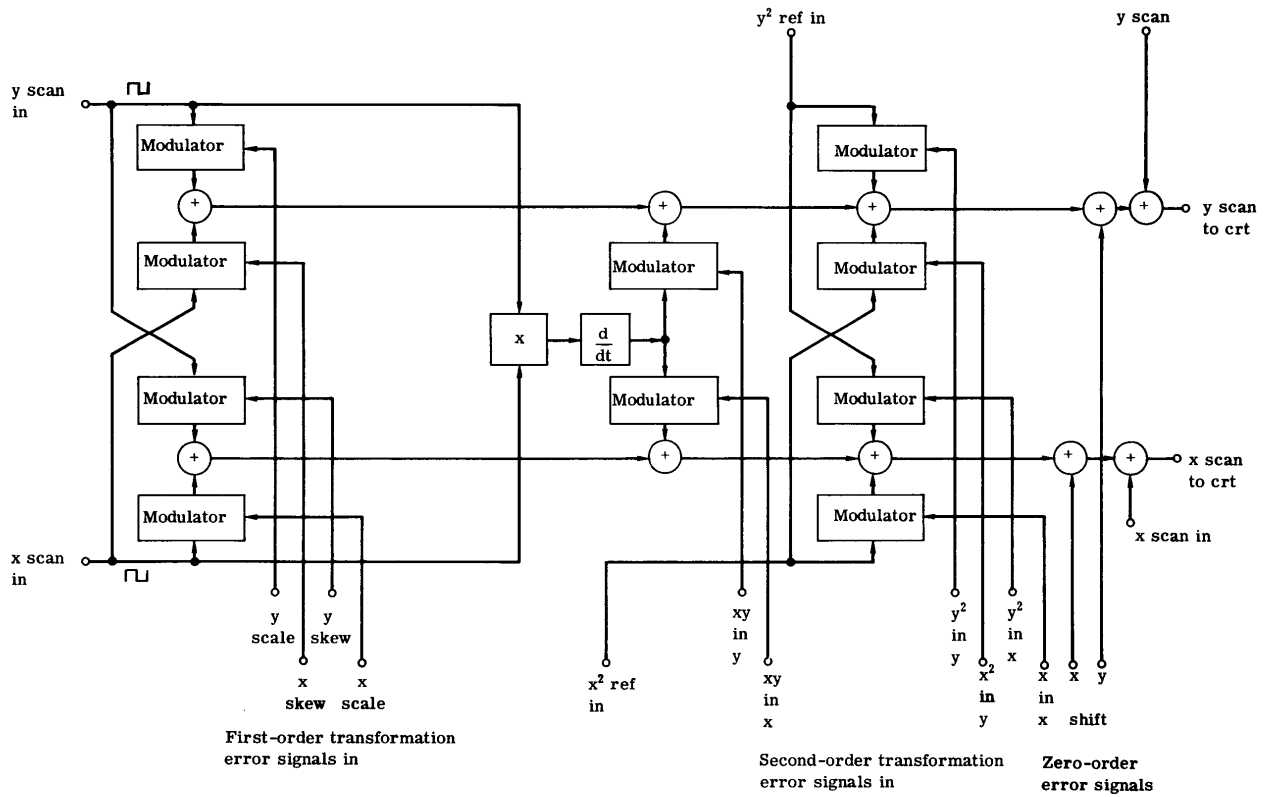


Fig. 3-9 — Block diagram of modulator circuits



The first stage of the processor is a wideband video amplifier feedback pair which steps up the video voltage to the level required by the gamma correction amplifier stages. The block diagram of a variable gamma amplifier used in our breadboard tests is shown in Fig. 3-11. As shown in Fig. 3-11, the video amplifier drives two gamma (nonlinear) amplifiers in parallel. One amplifier produces a video signal which is the square of the input, the other delivers a video signal output which is the square root of the input. To establish a constant operating point, a keyed dc clamp is provided, which sets the operating point (base bias) for the two gamma amplifiers during the blanking period, which is itself established by turning off the illumination on the flying spot tube during the turnaround of the scan cycle.

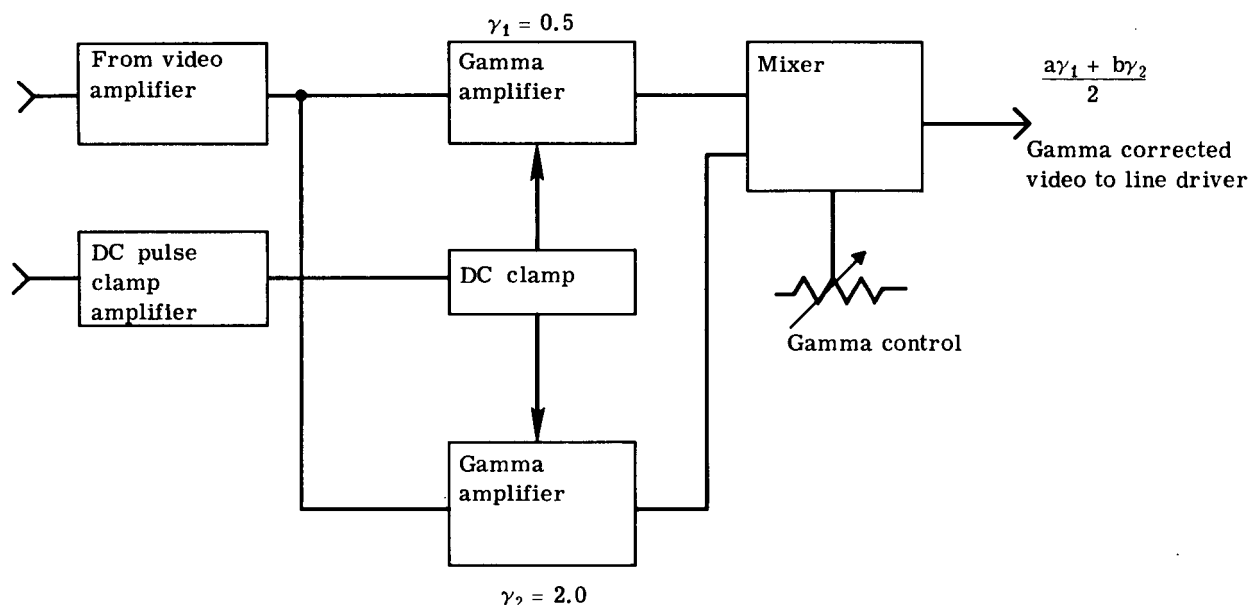


Fig. 3-11 — Block diagram of variable gamma amplifier

The nonlinear load for the gamma amplifiers is made up of three resistors in parallel, with diodes in series with two of the resistances, as shown in Fig. 3-12. The diodes are biased so that they close at different predetermined video signal levels, switching in the shunt resistance. Since the gain of the amplifier is proportional to the load resistance, this shunting effect lowers the load as the video signal increases, producing a close approximation to the desired nonlinear square root characteristic. Fig. 3-13 shows the transfer function characteristics of the nonlinear amplifier; for square law amplification the diode polarities are reversed.

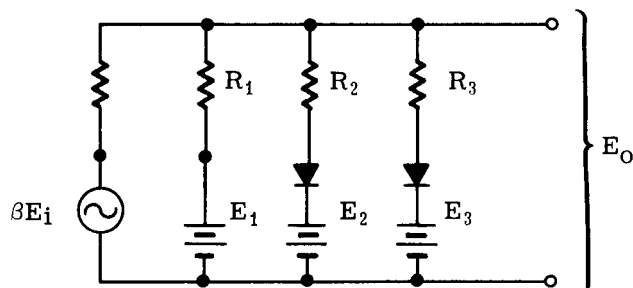


Fig. 3-12 — One form of nonlinear amplifier



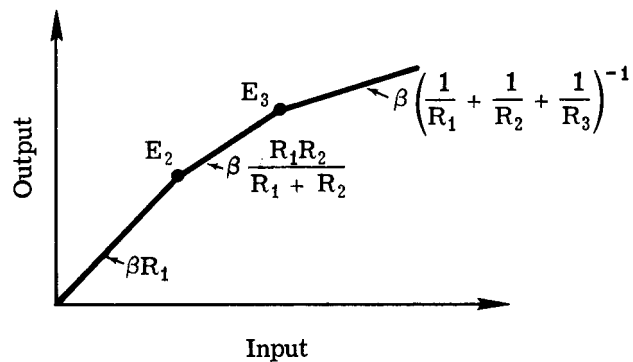


Fig. 3-13 — Transfer characteristic of nonlinear amplifier

The outputs of the two gamma amplifiers are fed to two inputs of a mixer, essentially two differential amplifiers. The signals are introduced into the emitters of each pair. One collector of each pair is tied together to a common load. A variable dc control bias applied to the base of a transistor in each of the differential amplifier pairs controls the amount of signal from each source. The output of the mixer has an approximately constant amplitude

$$\frac{a\gamma_1}{2} + \frac{b\gamma_2}{2} = k$$

where  $a$  and  $b$  are the amplitudes of the two gamma corrected signals as set by the gamma control bias, and  $k$  is a constant. It can be seen that at one end of the gamma control the output is  $\gamma_1$ , and at the other end it is  $\gamma_2$ . In the middle of the gamma control, the sum of the two signals closely approximates a linear signal.

The signal from the gamma correcting stages is fed to an aperture corrector. As shown in the general discussion of the MTF of the system (Section 2.3), the limit on resolution is in part imposed by the finite size of the scanning aperture. The falloff in MTF caused by aperture losses is phaseless, and is similar in character to the falloff in optical systems. It is possible to partially compensate for this effect by generating a rising, phaseless response characteristic as the video frequency increases in the video amplifier.

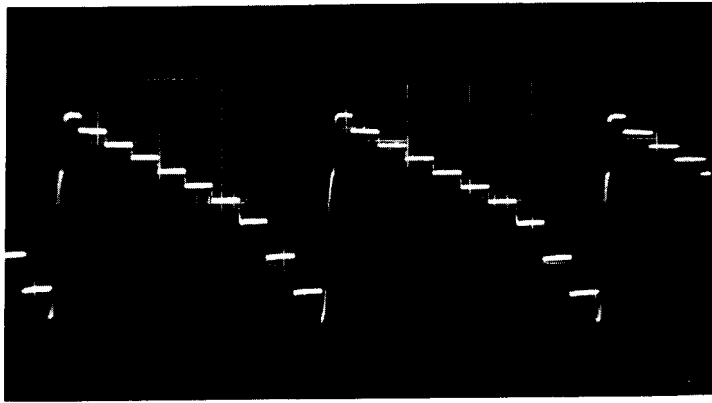
The amount of correction that can be introduced is limited by the increase in noise that can be tolerated. In general, it is safe to assume that an approximate 6 db boost can be used at the higher frequencies, resulting in an apparent increase in the sharpness of the reproduced picture. In our MTF analysis, the effect of the use of aperture correction was not included.

After being fed through the aperture correction circuitry, the signal is fed to the blanking insertion amplifier. The purpose of this stage is to insert a negative (black) pulse to blank the printout cathode-ray tube during the retrace of the scanning beam. Control of the amplitude of the blanking pulse is used to set the operating point on the monitor tubes.

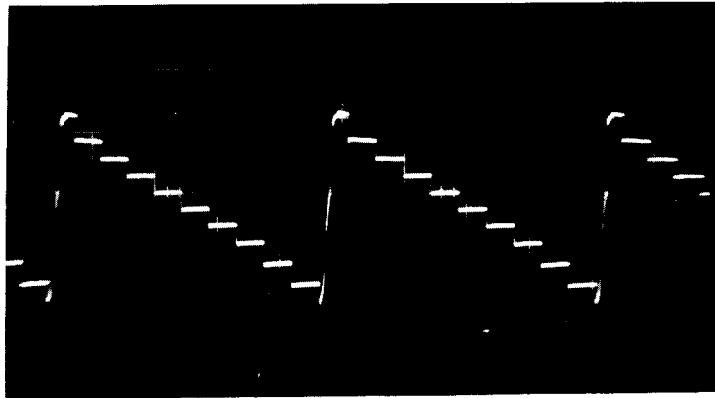
Fig. 3-14 shows the results obtained with a step voltage signal applied to the input of the gamma amplifier, and the gamma adjusted for each of the three conditions described.

Fig. 3-15a shows the waveform of a video signal with the positive peaks amplified more than the black, in essentially a square-law relationship. Fig. 3-15b results from taking the square root of the video signal with the black, negative peaks expanded.

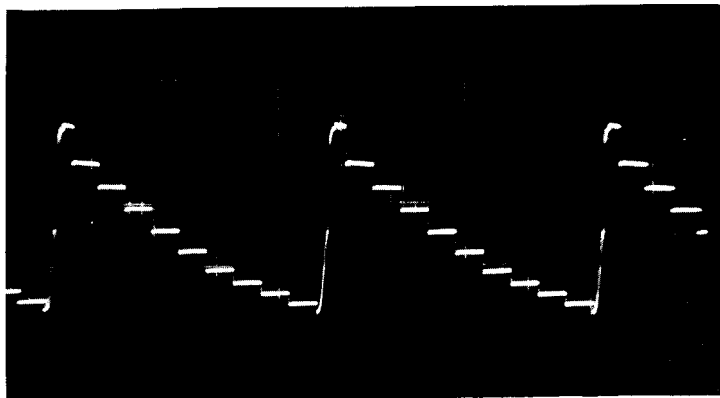
The effect, subjectively, of variable gamma control is that of illuminating the shadows for the rooting case, enhancing detail that previously was lost in more or less solid black.



(a) Signal A



(b) Signals (A + B)/2



(c) Signal B

Fig. 3-14 — Results of step voltage signal applied to input of gamma amplifier (0.5 ms/cm, 2 volts/cm)

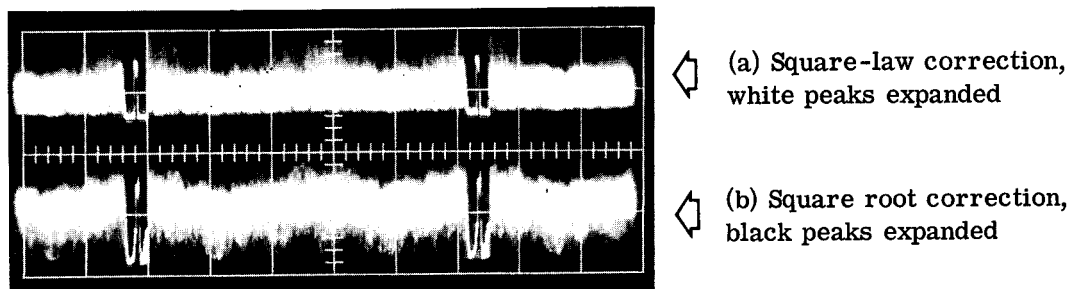


Fig. 3-15 — Video signals

### 3.5.2 Experimental Gamma Amplifier

The schematic of the experimental breadboard gamma amplifier is shown in Fig. 3-16. Two of these breadboards were constructed and used with the ARES for evaluation.

Tracing the circuit from the video input, which requires approximately 0.1 volt peak to peak of video signal, we see that the first two stages,  $Q_1$  and  $Q_2$ , comprise a feedback pair, with the gain adjustable by means of a resistance in the feedback loop. The output of this stage is fed to  $Q_3$  and  $Q_{10}$  in parallel, which are used to invert the signal before it is fed to the gamma amplifier driver,  $Q_5$ , in one channel, and  $Q_{11}$  in the other. The base of each of these stages is clamped, by a pulse derived from the blanking pulse on the flying spot tube, to the bias set by the potentiometer marked "black level adjust."

The nonlinear load for the gamma drivers is made up of three resistors in parallel. Two of the three resistors have diodes in series, biased such that the resistance is switched in as the video signal amplitudes overcome the bias voltage.

The outputs of the nonlinear amplifiers are coupled through emitter followers  $Q_5$  and  $Q_{11}$  to the adder stages,  $Q_6$  and  $Q_{12}$  in one channel, and  $Q_7$  and  $Q_8$  in the other. Each of these pairs is essentially a differential amplifier, with  $Q_6$  and  $Q_8$  sharing a common load. The two gamma corrected signals are applied to the common emitter load of each of the pairs. A dc bias controlled by the potentiometer marked "gamma" is applied to one base in each differential pair, so that as it is increased the amplitude of the signal from one pair increases, while the amplitude from the other decreases across the common load resistance. At one end of the gamma control setting, the video signal is solely from one channel; at the opposite end, from the other channel; and in the middle of the potentiometer setting, the two video signals are added in equal proportions.

The line driver consists of  $Q_{13}$ ,  $Q_{14}$ , and  $Q_{15}$ . Output gain is controlled by means of a control in the emitter of  $Q_{13}$ . Emitter  $Q_{15}$ , in series with  $Q_{16}$ , is the driver with a low source impedance, and permits the driving of several low impedance lines, as shown.

### 3.5.3 Video Combiner

The video signals from each of the three image dissector and video processor chains are fed to the video combiner. At this point, combinations of the three signals are made for purposes of registration in several modes: (1) superimposition, (2) flicker, and (3) individual image viewing.

The mode is selected by means of a switch on the control panel, and the result is viewed on the viewing monitor for the purpose of checking the registration before initiating the printout cycle.

Electronic Superimposition

Several modes of combining the images from each of the three film input stations will be provided. The simplest method of combining images electronically is by amplitude addition. Thus, the signal from station A is added to the signal from station B, and, if desired, the signal from station C is added to the first combination. One necessary technical consideration when planning the use of this method is the dynamic range of the video channel. When viewing one channel, the signal amplitude normally occupies the entire range (from black to white) that the video circuitry and the display cathode-ray tube can handle without saturation. It is therefore necessary that when signals are added together, the sum of their amplitudes be no greater than the amplitude of each video signal viewed separately. This requires that as signal B is added to signal A, the peak amplitude of signal A be reduced so that  $A + B = 1$ . Or, if  $B = A$ , A and B must both be reduced to one-half the amplitude that would be used if either were to be viewed independently. One signal can be subtracted from the other by reversing its polarity.

The overall effect of this type of addition is that each of the two images appears to have a lower brightness and contrast than when viewed independently. However, the capability of superimposition for purposes of registering several input sources is sufficiently valuable to warrant this sacrifice.

Several methods are available for automatically limiting the amplitude of the combined images to a value that prevents system overload. We will use a matrix that allows variable gain in each channel, while holding the output amplitude constant for all amplitudes of input.

Flicker

Another method of superimposition is the addition of the several signals in time. Each signal is gated independently into the display system in sequence. If it were possible to do this at a cyclic rate exceeding the eye's flicker sensitivity, the results obtained would be similar to the effects obtained by the amplitude additive method described above. The time additive technique is based on a law formulated by Fox Talbot in 1834:

"If a point of the retina is excited by a light which undergoes regular and periodic variations, and which has the duration of its period sufficiently short, it produces a continuous impression equal to that produced if the light emitted during each such period were distributed equally throughout the duration of the period."\*

In the design of television systems, flicker is avoided by presenting successive pictures to the eye at a rate well above that at which flicker is noticeable. However, if two images that are similar except for several small details are gated on in time sequence, and a balance is achieved for the larger tonal areas, the resulting image will appear to be continuous except for those small details that exist in only one image. These points will be presented at half the normal periodicity and will flicker at a rate that makes them very noticeable to the observer. By means of this method, successive photographs of the same area over a period of time can be quickly compared for the purpose of detecting new targets or other changes in an area of interest.

To make fullest use of this technique, several conditions must be met in the design of the electronic display system. These conditions relate to the geometry of the superimposed pictures, the luminance values of similar areas in each image, and the repetition rate at which each image is presented to the observer.

---

\*J. W. T. Walsh, "Photometry" 2nd ed., Constable and Co. Ltd, London, 1953, p. 67.



These conditions are interrelated. The repetition rate at which each image is flickered or gated into the display system is, for optimum detection, dependent on the luminance of the display. For low light levels, the critical frequency of flicker is much less than for displays of high luminance. The color of the display and the angle of view are also factors. The simplest case comprises periods of stimulation by a constant brightness alternating with equal periods of complete darkness. The lowest frequency at which no flicker is seen is defined as the critical frequency. Although this point varies from one observer to the next, at a luminance of approximately 1.0 foot-lambert, it is usually found to be between 12 and 15 flashes per second. A difference in luminance of  $1\frac{1}{2}$  percent between the two images is detectable at these frequencies.

From the above discussion it may be readily seen that the luminance of the two images to be analyzed must be adjusted such that the luminance of similar areas on the display screen differs by less than  $1\frac{1}{2}$  percent. The requirement for precise geometrical registration is necessitated by the fact that misregistered points will flicker.

Because of the characteristics of the electronic display system, it is necessary to select flicker rates that permit the display of an integral frame, or a multiple of integral frames, during the "on" period. Since the television frame rate is 30 cycles per second (60 fields interlaced 2 to 1) we can choose an "on" period of any integral multiple of  $1/30$  second. With one cycle representing the viewing of the two time-superimposed images, this limits us to flicker rates of 15, 7.5, 3.75, and 3 cycles, etc.

It is not recommended that flicker rates be chosen to include an odd number of fields per cycle, since interline flicker between the interlaced fields will be annoying during observation of fine detail and may have somewhat the same effect as geometrical misregistration of the images.

The flicker display mode is implemented by an electronic switch. Switching occurs during the period used for vertical retrace on the display screen, and is initiated by appropriate logic circuitry that is triggered by the vertical drive pulse. Selection of flicker rate will be on an individual channel basis that permits the operator to select the time during which each channel will be "on" in any integral number of frame periods. For example, it will be possible to switch channel A on for two frame periods and channel B on for one, by setting the channel A switch to 2 and the channel B flicker control switch to 1.

The flicker rate is variable in submultiples of the frame rate and is controlled by an electronic counter locked to the Lissajous scan converter. The output of the electronic counter operates an electronic switch in each channel. Fig. 3-17 shows the switching of two signals. For the purposes of illustration, one input signal is a 1-megacycle sine wave, the other a noise signal.

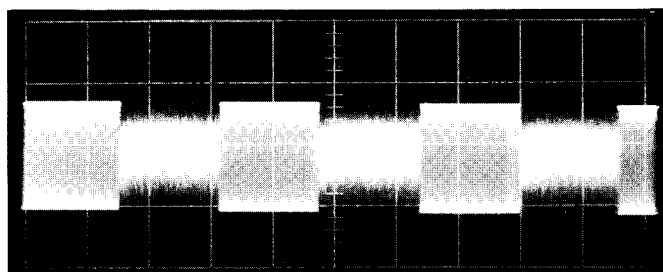


Fig. 3-17 — Switching for flicker presentation (0.2 ms/cm, 1 volt/cm)

The rate of the switching for flicker presentation is controlled by the counter which is locked to the frame time of the scan generator. The shortest duration of switching is one frame time. The duration can be selected in multiples of the frame time. This allows the duration selected

to be 1/30, 1/15, 1/8, 1/4, or 1/2 second. Thus, when two channels are being viewed, the flicker rate can be varied from 15 cps down to 1 cps. It is also possible to select different periods for each channel, so that, for example, one channel is viewed for two frames, and the other for one. In addition to the variable flicker rate, permanent on and off positions are provided on each control. By this means, one channel at a time may be flickered on on top of a continuous display by the remaining channels. This method of control is very flexible and avoids the display of incomplete frames.

### 3.6 SYSTEM PERFORMANCE

The expected performance of the complete multiple image integration viewer-printer system is summarized below.

#### 3.6.1 Input Material

The viewer will accept three film chips of any size up to 9 1/2 by 9 1/2 inches—positive, negative, or mixed.

#### 3.6.2 Hard Copy Output

The output will consist of a 3- by 3-inch image recorded on standard 4- by 5-inch cut film or Polaroid material. A regular 4- by 5-inch camera back will be used.

#### 3.6.3 Viewing Outputs

In addition to the film output, two viewing outputs will be provided for monitoring purposes:

1. A 10-inch-diagonal, short persistence crt scanned with the 500-line crossed diagonal raster, at 30 frames per second, to check operation of the automatic registration circuitry and to facilitate superimposition and gray scale adjustments
2. A 10-inch-diagonal, long persistence crt scanned with the 4,000-line, high resolution raster, at about 1 frame per second, to check operation of the slow scan readout and output image quality.

#### 3.6.4 Magnification Ratios

Three magnification ratios will be provided as detailed in Table 3-1. In addition, the size of each input will be electronically adjustable over a range of 2:1, to accommodate variations in image scale and geometry.

Table 3-1 — Input Magnification Ratios

Magnification Onto Film	Magnification Onto Viewing CRT's	Image Area Viewed at Input, inches
12×	28×	0.25 by 0.25
6.7×	15.5×	0.45 by 0.45
3.7×	8.6×	0.80 by 0.80

#### 3.6.5 Resolution

Modulation transfer functions of the complete system have been calculated and are shown in Figs. 3-18 and 3-19. Fig. 3-18 shows the individual MTF's of the basic components of the system,

all referred to the face of the image dissector tube. Fig. 3-19 shows the overall theoretical MTF of the complete system at the three magnification ratios of Table 3-1, referred to the input.

### 3.6.6 Signal to Noise Ratio

The signal to noise ratio of the system will be at least 100:1 (40 db). The signal to noise ratio of the output image will theoretically be increased by a factor of 1.73 over that of a single input when three inputs containing random additive noise with identical signal to noise ratios are integrated.

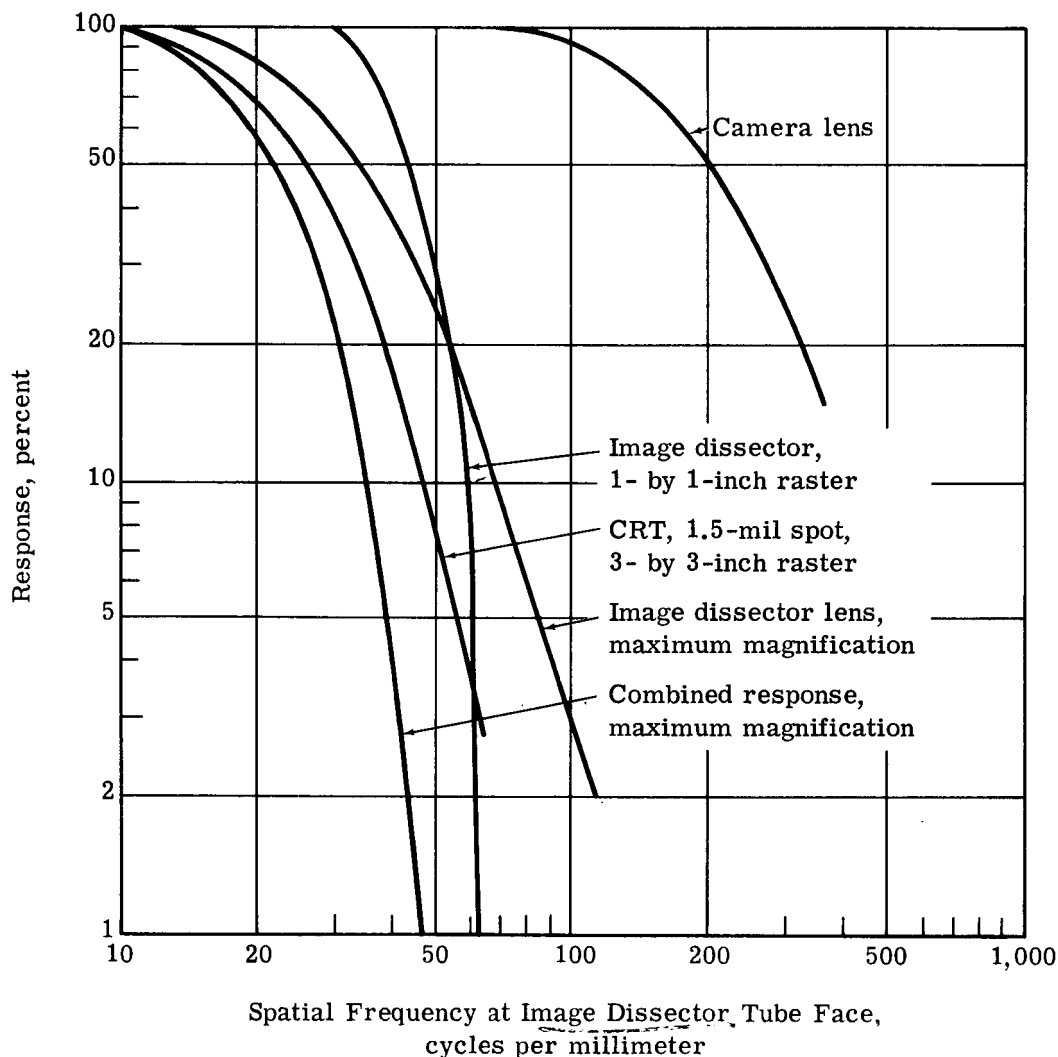


Fig. 3-18 — Modulation transfer functions referred to image dissector



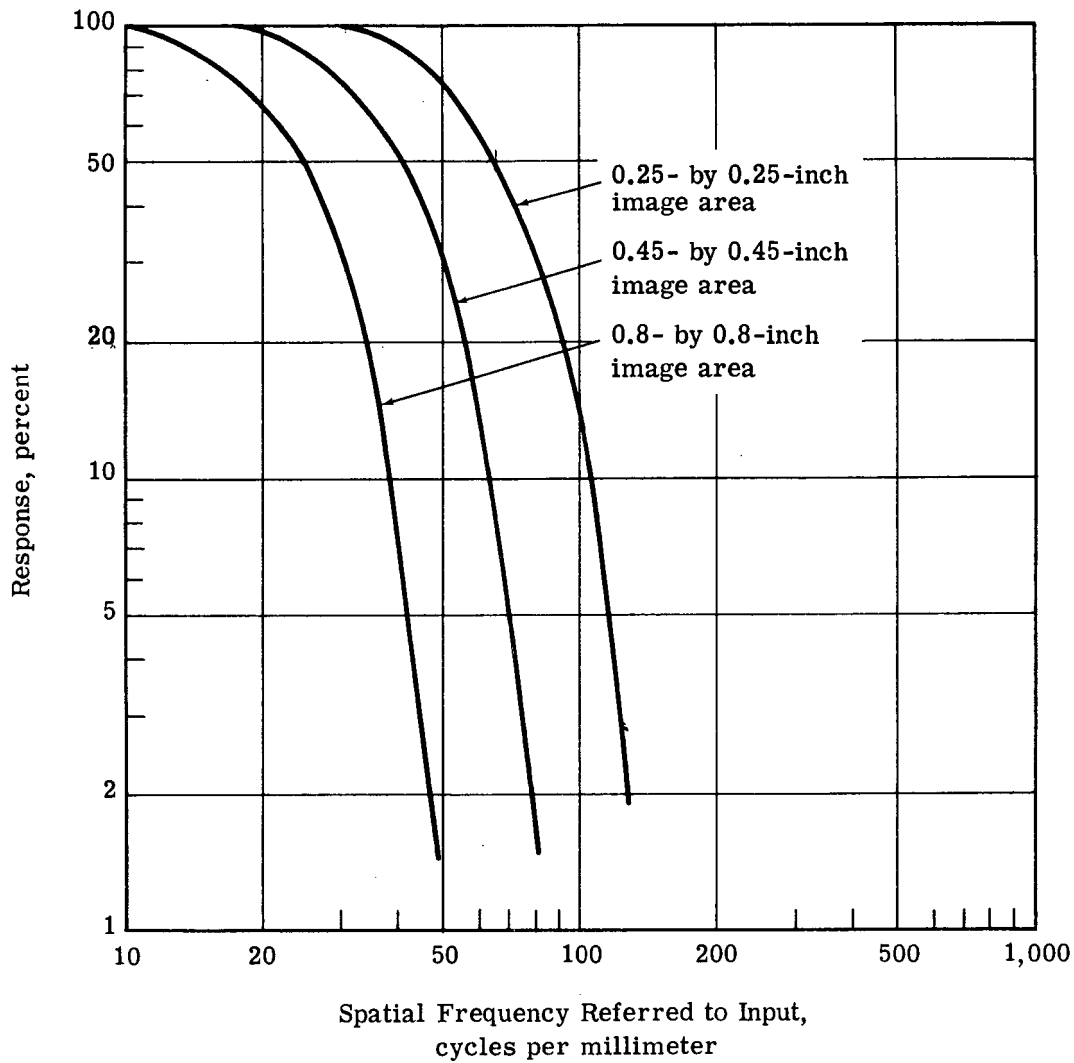


Fig. 3-19 — Theoretical modulation transfer function of complete system

4. BIBLIOGRAPHY

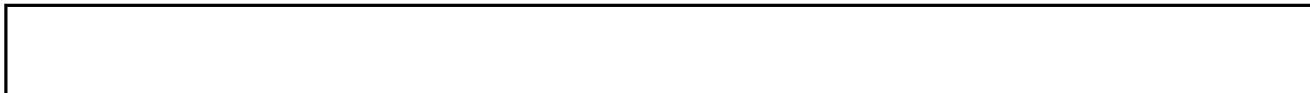
STAT

1. American Society of Photogrammetry, "Manual of Photogrammetry," George Banta Publishing Company, Menasha, Wisconsin, 1952, pp. 319-324, 336-345.
2. Perkin-Elmer Corporation, The Practical Application of Modulation Transfer Functions, Phot. Sci. Eng., 9(4):235-264 (July-Aug 1965).

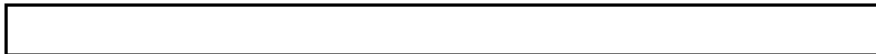


8. Scott, F., Scott, R. M., and Shack, R. V., The Use of Edge Gradients in Determining Modulation-Transfer Functions, Phot. Sci. Eng., 7(6):345-349 (Nov-Dec 1963).
9. Swing, R. E. and Shin, M. C. H., The Determination of Modulation-Transfer Characteristics of Photographic Emulsions in a Coherent Optical System, Phot. Sci. Eng., 7(6):350-360 (Nov-Dec 1963).
10. Wentworth, J. W., Color Television Engineering, RCA Victor Division, Radio Corporation of America, Apr 1962, pp. 7-8-7-13.

STAT



12. Kohler, R. J., and Howell, H. K., Photographic Image Enhancement by Superimposition of Multiple Images, Phot. Sci. Eng., 7(4):241-245 (July-Aug 1963).
13. Higgins, G. C., Lamberts, R. L., and Wolfe, R. N., Measurement and Analysis of the Distribution of Energy in Optical Images, J. Opt. Soc. Am., 48(7):487-490 (July 1958).
14. Lambert, R. L., Relationship Between the Sine-Wave Response and the Distribution of Energy in the Optical Image of a Line, J. Opt. Soc. Am., 48(7):490-495 (July 1958).
15. Lamberts, R. L., Application of Sine-Wave Techniques to Image-Forming Systems, J. SMPTE, 71(9):635-640 (Sept 1962).



STAT

## Appendix

## LINEAR SUPERIMPOSITION OF MULTIPLE IMAGES

## 1. GENERAL ANALYSIS

It is supposed that a number,  $N$ , of photographs containing the same signal,  $y$ , are to be superimposed so that the output,  $S$ , is

$$S = \sum_{i=1}^N \alpha_i (a_i y + n_i)$$

where  $a_i$  represents the signal amplitude and  $n_i$  represents the noise signal on the  $i^{\text{th}}$  input. The problem is to determine the coefficients,  $\alpha_i$ , to maximize the fidelity of the representation,  $S$ .

In optical signals, the dc noise level represents an overall gray scale and can result in a reduction of contrast. The detail, however, is not affected by the dc levels; it is degraded only by variations in the noise signal. The method employed here is to determine the  $\alpha_i$ 's so that the resultant noise variance is minimized for a given output signal strength.

The expression for the output can be rewritten as

$$S = \sum_{i=1}^N \beta_i \left( y + \frac{n_i}{a_i} \right)$$

where  $\beta_i = \alpha_i a_i$

The output signal strength is then fixed by constraining the  $\beta_i$ 's so that

$$\sum_{i=1}^N \beta_i = k$$

Let  $\sigma_i^2$  be the variance of the  $i^{\text{th}}$  noise signal. By noting that the variance of the noise signal,  $\beta_i n_i / a_i$ , is  $\beta_i^2 \sigma_i^2 / a_i^2$ , and using the fact that the variances of the different inputs add (because of the independence of the noise samples), we can write the variance of the output as

$$\sigma^2 = \sum_{i=1}^N \frac{\beta_i^2 \sigma_i^2}{a_i^2}$$

Using the Lagrange multiplier,  $\lambda$ , to take care of the constraint, we obtain

$$\sigma^2 = \sum_{i=1}^N \frac{\beta_i^2 \sigma_i^2}{a_i^2} - \lambda \left( \sum_{i=1}^N \beta_i - k \right)$$

Minimizing with respect to a particular coefficient, say  $\beta_j$ , we have

$$\delta \sigma^2 = \left( \frac{2\beta_j \sigma_j^2}{a_j^2} - \lambda \right) \delta \beta_j = 0$$

Since  $\delta \beta_j$  is arbitrary, the function in the parentheses must vanish, and the result is

$$\beta_j = \frac{a_j^2 \lambda}{2\sigma_j^2}$$

The value of  $\lambda$  can now be found from the constraint equation

$$\sum_{i=1}^N \beta_i = \frac{\lambda}{2} \sum_{i=1}^N \frac{a_i^2}{\sigma_i^2} = k$$

or

$$\lambda = \frac{2k}{M}$$

where

$$M = \sum_{i=1}^N \frac{a_i^2}{\sigma_i^2}$$

It should be noted that  $M$  can be determined from the inputs alone. The solution then is

$$\beta_i = \frac{k}{M} \times \frac{a_i^2}{\sigma_i^2}$$

or

$$\alpha_i = \frac{k}{M} \times \frac{a_i}{\sigma_i^2}$$

From this last expression it is seen that the variance of the output is minimized for a given output signal amplitude when the coefficients  $\alpha_i$  are proportional to the input signal strengths,  $a_i$ , and inversely proportional to the noise variances,  $\sigma_i^2$ . The constant  $k/M$  determines the intensity of the output and need not be computed in practice.

In the particular case of equal input signal amplitudes,  $a_i = a$ , and equal noise variances,  $\sigma_i^2 = \sigma^2$ , the result becomes

$$\alpha_i = \frac{k}{M} \times \frac{a}{\sigma^2} = \text{constant}$$

The coefficients  $\alpha_i$  and  $a_i$  then become superfluous and a single input can be represented by

$$y + n_i$$

By simply averaging the  $N$  inputs, we obtain the output

$$S = y + N \sum_{i=1}^N N_i$$

Since the noise samples are independent, the variance of the sum is the sum of the variances. The output variance, therefore, is

$$\sigma_o^2 = \frac{1}{N^2} \sum_{i=1}^N \sigma^2 = \frac{\sigma^2}{N}$$

and the standard deviation from average of the output noise signal is

$$\sigma_o = \frac{\sigma}{N^{1/2}}$$

Hence, in the case of equal input signal strengths and equal noise variances, the noise attenuation factor is the square root of the number of inputs.

## 2. SIGNAL TO NOISE RATIO

Having found the  $\alpha_i$ 's, we can find the output signal to noise ratio in terms of the input signal amplitudes,  $a_i$ , and the input noise variances,  $\sigma_i^2$ . The output is

$$S = \frac{k}{M} \sum_{i=1}^N \left( \frac{a_i^2}{\sigma_i^2} y + \frac{a_i N_i}{\sigma_i^2} \right)$$

The signal power is the integral of the square of the signal part of the output

$$\begin{aligned} P_S &= \frac{k^2}{M^2} \iint \left( \sum_{i=1}^N \frac{a_i^2}{\sigma_i^2} y(\xi, \eta) \right)^2 d\xi d\eta \\ &= \frac{k^2}{M^2} \left( \sum_{i=1}^N \frac{a_i^2}{\sigma_i^2} \right)^2 T \end{aligned}$$

where T is a constant given by

$$T = \iint y^2(x, y) dx dy$$

The noise power is the integral of the square of the noise part of the output

$$P_n = \frac{k^2}{M^2} \iint \left( \sum_{i=1}^N \frac{a_i}{\sigma_i^2} \eta_i(\xi, \eta) \right)^2 d\xi d\eta$$

When the dc components of noise are neglected, the above expression can be simplified by noting that all cross product terms in the square sum represent cross correlations of independent noise samples and hence integrate to zero. Therefore,

$$P_n = \frac{k^2}{M^2} \sum_{i=1}^N \left( \frac{a_i^2}{\sigma_i^4} \iint N_i^2(x, y) dx dy \right)$$

The power ratio of signal to noise then is

$$\frac{P_s}{P_n} = T \sum_{i=1}^N \frac{a_i^2}{\sigma_i^2}$$

In the case of equal input signal amplitudes and equal noise variances, the above expression becomes

$$\frac{P_s}{P_n} = NT \frac{a^2}{\sigma^2}$$

The amplitude signal to noise ratio is the square root of  $P_s/P_n$

$$R_N = \frac{A_s}{A_n} = T^{1/2} \left( \sum_{i=1}^N \frac{a_i^2}{\sigma_i^2} \right)^{1/2}$$

where the subscript N indicates that it is the ratio based on N inputs. If an additional input having signal amplitude  $a_{N+1}$  and noise variance  $\sigma_{N+1}^2$  is added, the new signal to noise amplitude ratio is given by

$$R_{N+1} = R_N^2 + \frac{a_{N+1}^2}{\sigma_{N+1}^2} T$$

It is apparent that no input can degrade the output. The worst possible case is encountered for an input having zero signal amplitude, in which case it is added in with zero weight and

$$R_{N+1} = R_N$$

In the case of equal input signal amplitudes and equal noise variances

$$R_N = \frac{a}{\sigma} (NT)^{1/2}$$